DISCRETE POINCARÉ INEQUALITY AND DISCRETE TRACE INEQUALITY IN PIECE-WISE POLYNOMIAL HYBRIDIZABLE SPACES

YUKUN YUE

ABSTRACT. In this paper, we establish discrete versions of the Poincaré and trace inequalities for hybridizable finite element spaces. These spaces are made of piecewise polynomial functions defined both within the interiors of elements and across all faces in a mesh's skeleton, serving as the basis for both the hybridizable discontinuous Galerkin (HDG) and hybrid high-order (HHO) methods. Additionally, we present a specific adaptation of these inequalities for the HDG method and apply them to demonstrate the stability of the related numerical schemes for second-order elliptic equations under the minimal regularity assumptions for the source term and boundary data.

1. INTRODUCTION

We take Ω as a connected, bounded, open polyhedral domain within $\mathbb{R}^d$, where d is either 2 or 3. $H^1(\Omega)$ denotes the standard Sobolev space consisting of functions in $L^2(\Omega)$ (the set of square integrable functions over Ω) whose first-order distributional derivatives are also in $L^2(\Omega)$. The classical Poincaré-Friedrichs inequalities for H^1 functions are outlined as follows [52, 66]:

$$\|f\|_{L^2(\Omega)}^2 \lesssim \|\nabla f\|_{L^2(\Omega)}^2 + \left(\int_\Omega f\,dx\right)^2 \qquad \forall f \in H^1(\Omega), \tag{1.1}$$

and

$$\|f\|_{L^2(\Omega)}^2 \lesssim \|\nabla f\|_{L^2(\Omega)}^2 + \left(\int_\Gamma f\,ds\right)^2 \qquad \forall f \in H^1(\Omega). \tag{1.2}$$

where Γ represents a measurable subset of $\partial\Omega$ with a positive $(d-1)$-dimensional measure. Additionally, the classical trace inequality is presented as follows [35, 41]:

$$\|f\|_{L^2(\partial\Omega)}^2 \lesssim \|f\|_{H^1(\Omega)}^2. \tag{1.3}$$

Applying the Poincaré-Friedrichs inequalities from (1.1) to (1.2), the trace inequality is thus reformulated as:

$$\|f\|_{L^2(\partial\Omega)}^2 \lesssim \|\nabla f\|_{L^2(\Omega)}^2 + \left(\int_\Omega f\,dx\right)^2 \qquad \forall f \in H^1(\Omega), \tag{1.4}$$

and

$$\|f\|_{L^2(\partial\Omega)}^2 \lesssim \|\nabla f\|_{L^2(\Omega)}^2 + \left(\int_\Gamma f\,ds\right)^2 \qquad \forall f \in H^1(\Omega). \tag{1.5}$$

Our primary focus is on extending these inequalities from the classical H^1 space to piecewise polynomial hybridizable spaces, given their significance in the mathematical analysis of partial differential equations (PDEs) [41, 44, 66]. These spaces have increasingly become prevalent in the spatial discretization of a variety of problems, thanks to the advent of several modern numerical methods. Notably, hybridizable discontinuous Galerkin (HDG) methods [14, 15, 17, 19, 22, 26, 38, 43, 55, 59] and hybrid high-order (HHO) methods [6, 12, 18, 28, 31, 33, 34, 36, 37] have been instrumental in this development.

The key distinction between hybridizable spaces and other more traditional nonconforming spaces [1, 10, 13, 27], often utilized in the discontinuous Galerkin (DG) method, is depicted in Figure 1. In the DG method, the approach involves using piecewise polynomial functions; for instance, as illustrated in the left part of

Date: March 29, 2024.

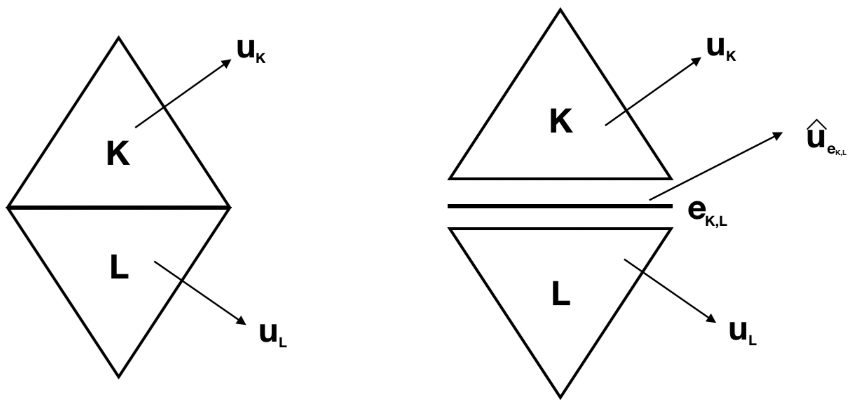

FIGURE 1. Comparison of Spaces: Nonconforming Space for DG Method (Left) versus Hybridizable Space for HDG or HHO Method (Right)

Figure 1, distinct functions u_K and u_L are selected for elements K and L respectively, and these functions may be discontinuous across the boundary where the two elements meet. Conversely, within hybridizable spaces, the function values are not only determined within the elements' interiors but also the function values on the boundaries are treated as separate variables. This idea is represented in the right part of Figure 1, where u_K and u_L are defined within elements K and L respectively, and $\hat{u}_{e_{K,L}}$ is defined on the interface $e_{K,L}$ between the two elements.

In recent years, significant efforts have been made to develop analogs of Poincaré-Friedrichs and trace inequalities as analytical tools for nonconforming spaces, which are extensively used in the analysis of various numerical methods. For further information, we direct readers to [7, 8, 11, 20, 42, 64, 65] and references therein. Notably, [8] established a foundational discrete Poincaré inequality for piecewise H^1 functions, applicable across a wide range of nonconforming spaces used in DG methods. However, the direct application of these findings is insufficient in establishing numerical stability for HDG methods due to challenges in controlling the jump term. This issue will be discussed in more detail in Section 3.1 and Section 5.

In this paper, we introduce analogues of the Poincaré inequalities (1.1) to (1.2) for any pair of piecewise polynomial functions $(u_h, \hat{u}_h) \in \mathcal{X}_h^k$, where $\mathcal{X}_h^k$ represents the hybridizable space (the precise definition of $\mathcal{X}_h^k$ is provided in Section 2.1):

$$\|u_h\|^2_{L^2(\Omega;\mathcal{T}_h)} \lesssim (h_K)^2 |u_h|^2_{H^1(\Omega;\mathcal{T}_h)} + h_K \|u_h - \hat{u}_h\|^2_{L^2(\Omega;\partial\mathcal{T}_h)} + \left|\mathcal{L}_h^{\mathcal{CR}}(\bar{\hat{u}}_h)\right|^2_{H^1(\Omega;\mathcal{T}_h)} + \left(\int_\Omega \hat{u}_h \, dx\right)^2 \tag{1.6}$$

and

$$\|u_h\|^2_{L^2(\Omega;\mathcal{T}_h)} \lesssim (h_K)^2 |u_h|^2_{H^1(\Omega;\mathcal{T}_h)} + h_K \|u_h - \hat{u}_h\|^2_{L^2(\Omega;\partial\mathcal{T}_h)} + \left|\mathcal{L}_h^{\mathcal{CR}}(\bar{\hat{u}}_h)\right|^2_{H^1(\Omega;\mathcal{T}_h)} + \left(\int_\Gamma \hat{u}_h \, ds\right)^2. \tag{1.7}$$

In this context, u_h represents a function defined within the interior of each element, whereas $\hat{u}_h$ pertains to a function specified on the mesh's skeleton. The mesh-specific term h_K denotes the diameter of a simplex K in the mesh. The term $\mathcal{L}_h^{\mathcal{CR}}$ refers to a lifting operator that maps piecewise constant functions into piecewise linear functions within the Crouzeix-Raviart space, detailed further in Section 3.2. $\bar{\hat{u}}_h$ is a piecewise constant function representing the average of $\hat{u}_h$ across each face of the mesh. Additional details on this are provided in Section 3, while a comprehensive explanation of all other relevant notations is provided in Section 2.1.

Moreover, we develop analogues of the trace inequalities, from (1.4) to (1.5), for any pair of piecewise polynomial functions $(u_h, \hat{u}_h) \in \mathcal{X}_h^k$:

$$\|u_h\|^2_{L^2(\Omega;\partial\mathcal{T}_h^b)} \lesssim h_K |u_h|^2_{H^1(\Omega;\mathcal{T}_h)} + \|u_h - \hat{u}_h\|^2_{L^2(\Omega;\partial\mathcal{T}_h^b)} + (1 + h_K)|\mathcal{L}_h^{\mathcal{CR}}(\bar{\hat{u}}_h)|^2_{H^1(\Omega;\mathcal{T}_h)} + \left(\int_\Gamma \hat{u}_h \, ds\right)^2 \tag{1.8}$$

and

$$\|\hat{u}_h\|^2_{L^2(\Omega;\partial\mathcal{T}_h^b)} \lesssim h_K|u_h|^2_{H^1(\Omega;\mathcal{T}_h)} + \|u_h - \hat{u}_h\|^2_{L^2(\Omega;\partial\mathcal{T}_h^b)} + (1+h_K)|\mathcal{L}_h^{\mathcal{CR}}(\bar{\hat{u}}_h)|^2_{H^1(\Omega;\mathcal{T}_h)} + \left(\int_\Gamma \hat{u}_h\,ds\right)^2. \tag{1.9}$$

Our proof of both the Poincaré and trace inequalities relies on the work presented in [7] and [8]. By employing a Crouzeix-Raviart lifting, we bridge hybridizable spaces with traditional nonconforming spaces. This methodology facilitates the use of theories from [7] and [8], allowing us to eliminate jump terms. Consequently, this enables us to achieve an estimate of order $O(h_K)$, as opposed to $O(\frac{1}{h_K})$.

Another main contribution of this paper involves utilizing the Poincaré inequality, as detailed from (1.6) to (1.7), and the trace inequality, from (1.8) to (1.9), to prove the stability of second-order elliptic equations solved by the HDG formulation. This approach represents a variation on the proof technique found in [46], which relies on a translation argument stemming from (1.7) for establishing stability. In Section 5, we will provide a proof based on the mathematical tools developed in this work directly.

Specifically, the mixed formulation approach [3, 4, 5], which considers a vector-valued mesh function

$$\boldsymbol{p}_h = -\nabla u_h,$$

is often adopted in the standard HDG formulation for second-order elliptic equations [21, 22, 25, 61] to devise the numerical scheme. For each element K, given $(u_h, \hat{u}_h) \in \mathcal{X}_h^k$, one can determine $\boldsymbol{p}_h \in \boldsymbol{\mathcal{V}}_h^k$ as it satisfies the following relation:

$$(\boldsymbol{p}_h, \boldsymbol{q}_h)_K = (u_h, \nabla\cdot\boldsymbol{q}_h)_K - \langle \hat{u}_h, \boldsymbol{q}_h\cdot\boldsymbol{n}\rangle_{\partial K} \tag{1.10}$$

where $\boldsymbol{\mathcal{V}}_h^k$ is space of piecewise-polynomial vector-valued functions that will be defined in Section 2.1. Introducing such a variable typically leads to an energy term involving $\|\boldsymbol{p}_h\|^2_{\boldsymbol{L}^2(\Omega;\mathcal{T}_h)}$, as opposed to $\|\nabla u\|^2_{\boldsymbol{L}^2(\Omega;\mathcal{T}_h)}$, which is more commonly encountered in classical elliptic theory [41]. The specifics of this distinction will be elaborated in Section 5. As a result, we require a variation of the existing analytical tools, adapted for use with $\boldsymbol{p}_h$. In the last section of this paper, we introduce the following findings: The Poincaré inequality from (1.6) to (1.7) is revised as

$$\|u_h\|^2_{L^2(\Omega;\mathcal{T}_h)} \lesssim (1+(h_K)^2)\|\boldsymbol{p}_h\|^2_{\boldsymbol{L}^2(\Omega;\mathcal{T}_h)} + h_K\|u_h - \hat{u}_h\|^2_{L^2(\Omega;\partial\mathcal{T}_h)} + \left(\int_\Omega u_h\,dx\right)^2 \tag{1.11}$$

and

$$\|u_h\|^2_{L^2(\Omega;\mathcal{T}_h)} \lesssim \left(1+(h_K)^2\right)\|\boldsymbol{p}_h\|^2_{\boldsymbol{L}^2(\Omega;\mathcal{T}_h)} + h_K\|u_h - \hat{u}_h\|^2_{L^2(\Omega;\partial\mathcal{T}_h)} + \left(\int_\Gamma \hat{u}_h\,ds\right)^2. \tag{1.12}$$

The trace inequalities (1.8)-(1.9) can be written as

$$\|u_h\|^2_{L^2(\Omega;\partial\mathcal{T}_h)} \lesssim (1+h_K)\|\boldsymbol{p}_h\|^2_{\boldsymbol{L}^2(\Omega;\mathcal{T}_h)} + \|u_h - \hat{u}_h\|^2_{L^2(\Omega;\partial\mathcal{T}_h)} + \left(\int_\Gamma \hat{u}_h\,ds\right)^2 \tag{1.13}$$

and

$$\|\hat{u}_h\|^2_{L^2(\Omega;\partial\mathcal{T}_h)} \lesssim (1+h_K)\|\boldsymbol{p}_h\|^2_{\boldsymbol{L}^2(\Omega;\mathcal{T}_h)} + \|u_h - \hat{u}_h\|^2_{L^2(\Omega;\partial\mathcal{T}_h)} + \left(\int_\Gamma \hat{u}_h\,ds\right)^2. \tag{1.14}$$

These inequalities will serve as important tools for developing novel analytical theories for hybridizable finite element methods, such as the HDG method.

The rest of this paper is organized as follows: Section 2 lays the groundwork for our study, covering essential notations like domain discretization and function spaces, mesh assumptions throughout our analysis, key technical lemmas aiding in the proof of our main results, and an introduction to the Crouzeix-Raviart space due to its critical role in our analysis. The Poincaré inequality for hybridizable spaces will be established in Section 3, where an averaging technique and a lifting from piece-wise constant space to the Crouzeix-Raviart space will be developed as key preliminary steps for the proof. Section 4 will extend the discussion to trace inequalities, employing a similar approach to the Poincaré inequality proof by utilizing a Crouzeix-Raviart element to bridge hybridizable and classical nonconforming spaces. Finally, Section 5 applies these findings to investigate the stability of the HDG method for second-order elliptic equations, obtaining a variant of these inequalities specifically designed for the HDG method.

2. Preliminary

This section is dedicated to presenting the foundational preliminaries necessary for this paper. We will outline the notations and general assumptions frequently used throughout. Additionally, we will review several technical lemmas well-known in finite element analysis that will be applied in later discussions. A concise overview of the Crouzeix-Raviart space is also provided, due to its importance in our analysis.

2.1. **Notations and Assumptions.**

2.1.1. *Space Discretization.* Consider a domain Ω, which is an open connected polyhedral region in $\mathbb{R}^d$. Here, d can either be 2 or 3. We define $\mathcal{T}_h$ as a shape-regular triangulation of Ω. (The exact definition of shape-regularity will be given in Section 2.1.4) This means $\mathcal{T}_h$ consists of triangles when $d = 2$ and tetrahedrons for $d = 3$. Each simplex in the triangulation is denoted as K, and so the entire domain can be written as $\bar{\Omega} = \bigcup\limits_{K\in\mathcal{T}_h} K$. When we have a face e appearing as the intersection of two adjacent simplex, labeled as K^+ and K^- ($e = \overline{K^+}\bigcap\overline{K^-}$), this face e is called an interior face of the triangulation $\mathcal{T}_h$. The set of all such interior faces is noted as $\partial\mathcal{T}_h^i$. The faces that lie on the boundary are collected under $\partial\mathcal{T}_h^b$. Hence, all faces within $\mathcal{T}_h$ can be collectively described as $\partial\mathcal{T}_h = \partial\mathcal{T}_h^i \cup \partial\mathcal{T}_h^b$. We call the collection of all the faces in the mesh to be skeleton. Additionally, the outward normal vectors for the simplexes K^+ and K^- are represented by $\boldsymbol{n}^+$ and $\boldsymbol{n}^-$, respectively. However, in practice, we often drop the superscripts and simply use $\boldsymbol{n}$ to denote the outward normal vector for a simplex K at any given face.

Regarding the mesh size of the triangulation $\mathcal{T}_h$, we use h_K to indicate the diameter of a simplex K. This diameter is defined as the greatest distance between any two points within the simplex K.

2.1.2. *Function Spaces.* The spaces that we will repeatedly utilize are listed here. Boldface notation will be used to indicate vector-valued functions or their corresponding spaces. The set of square integrable functions over $\mathcal{T}_h$ within Ω is represented as $L^2(\Omega;\mathcal{T}_h)$. Similarly, square integrable functions on the face space, $\partial\mathcal{T}_h$, are denoted by $L^2(\Omega;\partial\mathcal{T}_h)$. When addressing the function space associated with a specific element K, we modify the second component of this notation to reflect the domain of that element. For instance, $L^2(\Omega;K)$, $L^2(\Omega;\partial K)$, and $L^2(\Omega;e)$ are used to represent the spaces of square integrable functions on K, on the boundary of K, and on a face e belonging to $\partial\mathcal{T}_h$, respectively. These spaces are defined with specific norms: for functions $u_h \in L^2(\Omega;\mathcal{T}_h)$ and $\hat{u}_h \in L^2(\Omega;\partial\mathcal{T}_h)$,

$$\|u_h\|_{L^2(\Omega;\mathcal{T}_h)} = \left(\sum_{K\in\mathcal{T}_h} \|u_h\|^2_{L^2(\Omega;K)}\right)^{\frac{1}{2}}, \qquad \|\hat{u}_h\|_{L^2(\Omega;\partial\mathcal{T}_h)} = \left(\sum_{K\in\mathcal{T}_h} \|\hat{u}_h\|^2_{L^2(\Omega;\partial K)}\right)^{\frac{1}{2}}$$

Moreover, when evaluating the L^2 norm of a function that is defined over the whole mesh that exists within the interior part of each element, specifically $u_h \in L^2(\Omega;\mathcal{T}_h)$, we can define its L^2 norm over the skeleton, $\partial\mathcal{T}_h$, as well, by considering its trace on each face. Specifically, for $u_h \in L^2(\Omega;\mathcal{T}_h)$, its norm on $\partial\mathcal{T}_h$ is expressed as $\|u_h\|_{L^2(\Omega;\partial\mathcal{T}_h)}$. This is detailed by the following equation:

$$\begin{aligned}\|u_h\|_{L^2(\Omega;\partial\mathcal{T}_h)} &= \left(\sum_{K\in\mathcal{T}_h} \|u_h\|^2_{L^2(\Omega;K)}\right)^{\frac{1}{2}} \\ &= \left(\sum_{e\in\partial\mathcal{T}_h^i} \|u_h\boldsymbol{n}_e^+\|^2_{L^2(\Omega;e)} + \sum_{e\in\partial\mathcal{T}_h^i} \|u_h\boldsymbol{n}_e^-\|^2_{L^2(\Omega;e)} + \sum_{e\in\partial\mathcal{T}_h^b} \|u_h\boldsymbol{n}_e\|^2_{L^2(\Omega;e)}\right)^{\frac{1}{2}},\end{aligned}$$

where $\boldsymbol{n}_e^+$ and $\boldsymbol{n}_e^-$ denote the outward normal vectors on each side of an interior face e, and $\boldsymbol{n}_e$ represents the outward normal vector at the boundary for a boundary face e. Therefore, u_h on each interior face is computed twice, reflecting the contributions from both sides of the face. $(\cdot,\cdot)_X$ will be used to denote inner product in $L^2(\Omega;X)$ when X is a collection of simplexes while we use $\langle\cdot,\cdot\rangle_X$ if X is one or a collection of faces.

We designate $H^1(\Omega;\mathcal{T}_h)$ to represent for piecewise H^1 functions which is defined as

$$H^1(\Omega;\mathcal{T}_h) = \left\{f \in L^2(\Omega;\mathcal{T}_h) : f_K = f|_K \in H^1(\Omega;K), \forall K \in \mathcal{T}_h\right\} \tag{2.1}$$

We will use the operator ∇_h to denote the broken gradient operator [58]. In this context, $\nabla_h f$ and $\nabla_h \cdot \boldsymbol{f}$ refer to functions that, when restricted to an element K, equal ∇f and $\nabla \cdot \boldsymbol{f}$, respectively. The semi-norm for $H^1(\Omega; \mathcal{T}_h)$ is given by

$$|f|_{H^1(\Omega;\mathcal{T}_h)} = \left(\sum_{K \in \mathcal{T}_h} \|\nabla u_h\|^2_{L^2(\Omega;K)} \right)^{\frac{1}{2}} = \|\nabla_h u_h\|_{L^2(\Omega;K)} \tag{2.2}$$

We want to clarify for readers that the notation $H^1(\Omega)$, which will be discussed in Section 4, refers to the standard Sobolev space. Regarding the L^2 space, it's important to note that $L^2(\Omega) = L^2(\Omega; \mathcal{T}_h)$ and $L^2(\partial\Omega) = L^2(\Omega; \partial\mathcal{T}_h)$. Therefore, we will not distinguish between these notations.

Next, we focus on defining the hybridizable spaces, which are central to this paper. The piecewise polynomial space $\mathcal{U}_h^k$ within the domain is delineated as follows:

$$\mathcal{U}_h^k = \{ f \in L^2(\Omega; \mathcal{T}_h) : f|_K \in \mathcal{P}^k(K), \forall K \in \mathcal{T}_h \}, \tag{2.3}$$

and the piecewise polynomial space $\mathcal{F}_h^k$ over the faces is outlined as:

$$\mathcal{F}_h^k = \{ \hat{f} \in L^2(\Omega; \partial\mathcal{T}_h) : \hat{f}|_e \in \mathcal{P}^k(\partial K), \forall e \in \partial\mathcal{T}_h \}. \tag{2.4}$$

Here, $\mathcal{P}^k$ denotes the collection of polynomials with degree at most k. The combined space, $\mathcal{X}_h^k$, is thus formulated as the Cartesian product of $\mathcal{U}_h^k$ and $\mathcal{F}_h^k$:

$$\mathcal{X}_h^k = \mathcal{U}_h^k \times \mathcal{F}_h^k. \tag{2.5}$$

Our analysis will primarily focus on elements within $\mathcal{X}_h^k$, denoted by $(u_h, \hat{u}_h) \in \mathcal{X}_h^k$. Additionally, we introduce the concept of a vector-valued piecewise polynomial function space, $\boldsymbol{\mathcal{V}}_h^k$, defined as:

$$\boldsymbol{\mathcal{V}}_h^k = \{ \boldsymbol{f} \in \boldsymbol{L}^2(\Omega; \mathcal{T}_h) : \boldsymbol{f}|_K \in \boldsymbol{\mathcal{P}}^k(K), \forall K \in \mathcal{T}_h \} \tag{2.6}$$

This space becomes relevant when employing a lifting operator to transform a scalar function, defined on the mesh skeleton, into a vector function that is defined on the entire mesh. More information on this will be provided in Section 5.1. Additionally, it will be used for the discussion on HDG formulations in Section 5.

2.1.3. *Other Notations.* To avoid proliferation of constants, we will use the notation $\lesssim$ in this paper. Specifically, when we say $f_1 \lesssim f_2$, it implies the existence of a constant $C > 0$, which is independent of both f_1 and f_2, ensuring $f_1 \leq C f_2$.

Additionally, we follow the standard notations for jump at the boundaries of elements consisting of piecewise continuous functions [9]. For a given function $f \in \mathcal{U}_h^k$, and a face e which is the boundary between two elements K^+ and K^- with respective outward normal vectors $\boldsymbol{n}^+$ and $\boldsymbol{n}^-$ (where $e = \overline{K^+} \bigcap \overline{K^-}$), the jump of f across face e is defined by the equation:

$$[[f]]_e = f^+ \boldsymbol{n}^+ + f^- \boldsymbol{n}^- \tag{2.7}$$

Here, f^+ and f^- indicate the values of f on the sides of K^+ and K^-, respectively.

We employ $|\cdot|$ to signify the magnitude or measure of an object. For instance, $|K|$ refers to the d-dimensional measure of K, while $|\partial K|$ and $|e|$ relate to the $(d-1)$-dimensional measures of ∂K and a face e, respectively. Based on the shape regularity assumption, which will be detailed in Section 2.1.4, we can assert that $|K| \propto (h_K)^d$ and $|\partial K| \propto (h_K)^{d-1}$.

For integral notation, we use dx when referring to spatial integrals and ds for integrals taken over faces. We also use $f|_K$ and $f|_e$ to denote the restriction of a function on a simplex K or a face e, respectively.

2.1.4. *Mesh Assumptions.* In this section, we establish certain mesh assumptions. These criteria are broadly applicable across a range of meshes and are commonly used in analyses of DG and HDG methods, as seen in [8, 23].

A1 (Shape Regularity Assumption): There exists a constant $\kappa_{\mathcal{T}} > 0$ such that for any mesh size $h_K > 0$, the minimum ratio of the volume of any simplex K within the mesh $\mathcal{T}_h$ to the power of its diameter (cubed for $d = 3$ or squared for $d = 2$) is always above $\kappa_{\mathcal{T}}$:

$$\min_{K \in \mathcal{T}_h} \frac{|K|}{\operatorname{diam}(K)^d} \geq \kappa_{\mathcal{T}}. \tag{2.8}$$

A2 (Hanging Node Assumption): The mesh does not contain hanging nodes.

Two remarks are given here regarding these assumptions:

Remark 2.1. The Shape Regularity Assumption (A1) introduces a constant $\theta_{\mathcal{T}} > 0$, which bounds the maximum diameter of any simplex K relative to the diameter of the largest inscribed sphere in K, for all $h > 0$:

$$\max_{K \in \mathcal{T}_h} \frac{\operatorname{diam}(K)}{\rho_K} \leq \theta_{\mathcal{T}},$$

where ρ_K represents the inscribed sphere's diameter. It also establishes a constant $\varphi_{\mathcal{T}} > 0$, ensuring the minimum angle within any simplex K remains above $\varphi_{\mathcal{T}}$. This angle is measured in radians for $d = 2$ or steradians for $d = 3$.

Remark 2.2. While our findings could be extended to more complex meshes, incorporating hanging nodes would overly complicate the paper's structure. Thus, we choose this assumption (A2) to focus on simplicial meshes, which more effectively illustrate our proof's core ideas.

2.2. **Technical Lemmas.** This section outlines several well-known results that pave the way for the proofs developed later in this paper. We begin with the discrete trace theorem in triangular simplex, summarized in the lemma below.

Lemma 2.3. Consider a simplex K in $\mathbb{R}^d$, with e representing one of its faces. For any function f belonging to $\mathcal{P}^k(K)$, the following inequality holds true:

$$\|f\|_{L^2(\Omega;e)} \leq \left(\frac{(k+1)(k+d)}{d}\right)^{\frac{1}{2}} \left(\frac{|e|}{|K|}\right)^{\frac{1}{2}} \|f\|_{L^2(\Omega;K)} \tag{2.9}$$

Proof. For the proof, we refer readers to [65][Theorem 5]. □

Remark 2.4. The lemma mentioned primarily focuses on scalar-valued functions. To extend this principle to vector-valued functions, one can evaluate the inequality for each vector component separately and then combine the results. This approach leads to a vector-valued version of the inequality.

Remark 2.5. Considering a simplex K and its face e, there is a proportional relationship between their measures, expressed as $|K| = c_d h_e |e|$. Here, h_e represents the height from face e within K, and c_d is only dependent on the dimension d. With h_K denoting the diameter of the simplex, the discrete trace inequality can be rephrased to reflect this geometrical relation under the shape regularity assumption, as follows:

$$\|f\|_{L^2(\Omega;e)} \lesssim \frac{1}{h_K^{\frac{1}{2}}} \|f\|_{L^2(\Omega;K)}. \tag{2.10}$$

Next, we present the Poincaré inequality in a simplex K, which includes an estimate of the order of the Poincaré constant in this case.

Lemma 2.6. Let K be a simplex, e is a face in ∂K, and $f \in H^1(\Omega; K)$. We set

$$f_e := \frac{1}{|e|} \int_e f \, ds, \qquad f_K = \frac{1}{|K|} \int_K f \, dx.$$

They denote the average of f over one face e and the interior of simplex K, respectively. Then the following estimates hold

$$\int_K (f_K - f_e)^2 \, dx \lesssim \operatorname{diam}(K)^2 \int_K |\nabla f|^2 \, dx, \tag{2.11}$$

$$\int_K [f - f_K]^2 \, dx \lesssim \operatorname{diam}(K)^2 \int_K |\nabla f|^2 \, dx. \tag{2.12}$$

and

$$\int_K [f - f_e]^2 \, dx \lesssim \operatorname{diam}(K)^2 \int_K |\nabla f|^2 \, dx. \tag{2.13}$$

Proof. See [64][Lemma 4.1] for (2.11) and (2.13) and then (2.12) will follow as a consequence. Or see [57] and [40] for (2.12) directly. □

This leads us to understand that the L^2 norm of the difference between a function and its mean value (either averaged over the entire simplex or just on one face of it) can be bounded by the function's H^1 semi-norm, multiplied by a constant that depends on the simplex's diameter.

2.3. **Crouzeix–Raviart Space.** Introduced by Crouzeix and Raviart in the early 1970s [27], the Crouziex-Raviart (CR) finite element space is an important development in the area of non-conforming P_1 finite elements. Characterized by its application to both triangular ($d = 2$) and tetrahedron ($d = 3$) cases, the CR space uniquely defines its degrees of freedom through the evaluation of functions at the midpoint of edges or faces. This distinctive approach results in element functions that maintain continuity exclusively at these midpoints, different from the traditional conforming elements [9, 16, 67] which are continuous across the entire element.

As a consequence, the discontinuity outside the midpoints of edges or faces makes CR finite element function not an element of the Sobolev space $H^1(\Omega)$ which is the standard space for second-order elliptic equations to be posed in [41, 44]. This difference underscores the non-conforming nature of the CR space. The theoretical analysis and evolution of CR space are extensively discussed in literature. We refer readers to [2, 10, 30, 45] and the references therein.

Here, we give the precise definition of the CR space:

$$\mathcal{CR}(\Omega; \mathcal{T}_h) = \{f \in L^2(\Omega; \mathcal{T}_h) : f|_K \in \mathcal{P}^1(K), \int_e [[f]]_e \, ds = 0 \text{ for all } e \in \partial\mathcal{T}_h^i\}. \tag{2.14}$$

The condition that the integral of the function's jump across any interior edge is zero underlines that the CR space's degrees of freedom are centered on the edges' midpoints. In this research, the CR space is utilized for the interpolation of a function $\hat{\mu}$, defined on the mesh skeleton, into a P_1 element within the CR space. The specifics of this interpolation method will be detailed in Section 3.2.

3. Discrete Poincaré Inequality

This section focuses on establishing one of our main results, the Poincaré inequality, within the hybridizable space $\mathcal{X}_h^k$. Our approach involves linking hybridizable spaces to DG spaces via a lifting operator. This connection is set up by utilizing the Crouzeix-Raviart element as an intermediary.

3.1. **Discrete Poincaré Inequality for Piecewise H^1 Functions.** To start, we revisit the discrete Poincaré-Friedrichs inequalities that applied to classical nonconforming finite element methods and discontinuous Galerkin methods, as introduced in [8]. These inequalities will serve as crucial tools in deriving the Poincaré-Friedrichs inequalities for hybridizable spaces.

Lemma 3.1. The following are the Poincaré–Friedrichs inequalities for $f \in H^1(\Omega; \mathcal{T}_h)$ where $H^1(\Omega; \mathcal{T}_h)$ is the space of piecewise H^1 functions defined in (2.1):

$$\|f\|^2_{L^2(\Omega;\mathcal{T}_h)} \lesssim \left[|f|^2_{H^1(\Omega,P)} + \sum_{e \in \partial\mathcal{T}_h^i} |e|^{d/(1-d)} \left| \int_e [[f]]_e \, ds \right|^2 + \left(\int_\Omega f \, dx \right)^2 \right], \tag{3.1}$$

$$\|f\|^2_{L^2(\Omega;\mathcal{T}_h)} \lesssim \left[|f|^2_{H^1(\Omega,P)} + \sum_{e \in \partial\mathcal{T}_h^i} |e|^{d/(1-d)} \left| \int_e [[f]]_e \, ds \right|^2 + \left(\int_\Gamma f \, ds \right)^2 \right], \tag{3.2}$$

where $|e|$ represents the $(d-1)$-dimensional measure of the face e, and $[[f]]_e$ signifies the jump of the function f across the face e, as defined in (2.7). The positive constant, not explicitly mentioned due to the use of the symbol $\lesssim$, relies solely on the shape regularity of the partition P. And Γ is a subset of $\partial\Omega$ that has a positive measure.

Proof. See [8]. $\square$

The following corollary is an immediate result when the integral of jump at each interior face vanishes, namely,

$$\int_e [[f]]_e \, ds = 0 \tag{3.3}$$

for every $e \in \partial\mathcal{T}_h^i$.

Corollary 3.2. If condition (3.3) holds, then (3.1)-(3.2) will reduce to

$$\|f\|^2_{L^2(\Omega;\mathcal{T}_h)} \lesssim |f|^2_{H^1(\Omega,P)} + \left(\int_\Omega f \, dx\right)^2, \tag{3.4}$$

and

$$\|f\|^2_{L^2(\Omega;\mathcal{T}_h)} \lesssim |f|^2_{H^1(\Omega,P)} + \left(\int_\Gamma f \, ds\right)^2. \tag{3.5}$$

For any function f within the CR space, as defined in (2.14), it satisfies the condition given in (3.3). Therefore, the two types of Poincaré-Friedrichs inequalities mentioned above, (3.4) and (3.5), which apply to cases without jumps in integral sense, are naturally applicable to a CR element.

We want to point out that Lemma 3.1 is broadly applicable and serves as a cornerstone in the theory of the DG method [32, 39, 47, 60]. This lemma allows us to generalize the concept of derivatives to discontinuous spaces and lays down a framework for designing a generalized gradient operator. It illustrates what gradients look like within such spaces. However, directly applying these principles to hybridizable spaces does not suffice to achieve the inequalities presented in (1.6)-(1.7). In fact, when considering an element $(u_h, \hat{u}_h) \in \mathcal{X}_h^k$, if the jump term $\sum_{e\in\partial\mathcal{T}_h^i} |e|^{d/(1-d)} \left|\int_e [[u_h]]_e \, ds\right|^2$ in (3.1) and (3.2) remains, the best estimate we could expect for this term would be

$$\sum_{e\in\partial\mathcal{T}_h^i} |e|^{d/(1-d)} \left|\int_e [[u_h]]_e \, ds\right|^2 \leq \sum_{e\in\partial\mathcal{T}_h^i} |e|^{1/(1-d)} \left|\int_e \left([[u_h]]_e\right)^2 \, ds\right| \lesssim \sum_{e\in\partial\mathcal{T}_h^i} h_K{}^{\frac{1}{1-d}} \|u_h - \hat{u}_h\|^2_{L^2(\Omega;e)}.$$

This is weaker than the estimates in (1.6)-(1.7), where we obtain a coefficient related to h_K of order $O(h_K)$ for this analog of the jump term. This observation suggests the need to eliminate the jump term $\sum_{e\in\partial\mathcal{T}_h^i} |e|^{d/(1-d)} \left|\int_e [[u_h]]_e \, ds\right|^2$ for a more accurate estimate, leading to the introduction of the CR lifting operator in the following subsection.

3.2. **CR Lifting Operator.** Here we introduce a lifting operator mapping a piece-wise constant function defined on skeleton of the mesh to be a function defined in the CR space. We define $\mathcal{L}_h^{\mathcal{CR}} : \mathcal{P}^0(\partial\mathcal{T}_h) \to \mathcal{CR}(\Omega;\mathcal{T}_h)$ as

$$\mathcal{L}_h^{\mathcal{CR}}(\hat{\mu})(c_e) = \hat{\mu}|_e \tag{3.6}$$

for every $\hat{\mu} \in \mathcal{P}^0(\partial\mathcal{T}_h)$ and face $e \in \partial\mathcal{T}_h$. Here c_e denotes the center of the face e and the left-hand side of (3.6) is to evaluate $\mathcal{L}_h^{\mathcal{CR}}(\hat{\mu})$ at point c_e. In other words, the lifting operator defines a CR element by determining its degree of freedom lying on the centers of each side of each element.

The following result describes the quantity relation between $\hat{\mu}$ and $\mathcal{L}_h^{\mathcal{CR}}(\hat{\mu})$ when it is restricted in K.

Lemma 3.3. We take the restriction of $\hat{\mu} \in \mathcal{P}^0(\partial\mathcal{T}_h)$ on an element K as $\hat{\mu}_K = \hat{\mu}|_K$, then

$$\|\hat{\mu}_K\|^2_{L^2(\Omega;\partial K)} \leq \|\mathcal{L}_h^{\mathcal{CR}}(\hat{\mu}_K)\|^2_{L^2(\Omega;\partial K)} = \|\mathcal{L}_h^{\mathcal{CR}}(\hat{\mu})|_K\|^2_{L^2(\Omega;\partial K)} \tag{3.7}$$

Proof. Consider a face e within ∂K and let $\hat{\mu}_{K,e}$ represent the value of μ on face e. We can express this term in another way as

$$\hat{\mu}_{K,e} = \frac{1}{|e|}\int_e \mathcal{L}_h^{\mathcal{CR}}(\hat{\mu}_K) \, ds$$

due to the linearity of $\mathcal{L}_h^{\mathcal{CR}}(\hat{\mu}_K)$ and the definition of the CR lifting operator. Applying the Cauchy-Schwarz inequality, we get

$$(\hat{\mu}_{K,e})^2 = \frac{1}{|e|^2}\left[\int_e \mathcal{L}_h^{\mathcal{CR}}(\hat{\mu}_K)\,ds\right]^2 \le \frac{1}{|e|}\int_e \left[\mathcal{L}_h^{\mathcal{CR}}(\hat{\mu}_K)\right]^2\,ds = \frac{1}{|e|}\left\|\mathcal{L}_h^{\mathcal{CR}}(\hat{\mu}_K)\right\|^2_{L^2(\Omega;e)} \tag{3.8}$$

Following this,

$$\|\hat{\mu}_K\|^2_{L^2(\Omega;\partial K)} = \sum_{e\in\partial K}|e|(\hat{\mu}_{K,e})^2 \le \sum_{e\in\partial K}\left\|\mathcal{L}_h^{\mathcal{CR}}(\hat{\mu}_K)\right\|^2_{L^2(\Omega;e)} = \|\mathcal{L}_h^{\mathcal{CR}}(\hat{\mu}_K)\|^2_{L^2(\Omega;\partial K)}$$

This concludes the proof. □

3.3. **Poincaré Inequalities in $\mathcal{X}_h^k$.** In this part, our goal is to prove the Poincaré inequalities for the space $\mathcal{X}_h^k$. Before proceeding with the proof, it's crucial to recognize that $\hat{u}_h \in \mathcal{F}_h^k$ is generally a $\mathcal{P}^k$ function, not a $\mathcal{P}^0$ function. For the CR lifting operator to be applicable, we need to transform these piecewise polynomial functions into piecewise constant ones. Thus, for a boundary face e and a function $\hat{u}_h \in \mathcal{F}_h^k$, we take:

$$\bar{\hat{u}}_{h,e} = \frac{1}{|e|}\int_e \hat{u}_h\,ds \tag{3.9}$$

Then $\bar{\hat{u}}_h \in \mathcal{P}^0(\partial\mathcal{T}_h)$ is introduced as a piecewise constant function that averages $\hat{u}_h$ on each boundary segment, defined by:

$$\bar{\hat{u}}_h|_e = \bar{\hat{u}}_{h,e} \tag{3.10}$$

This procedure converts $\hat{u}_h$ into the piecewise constant function $\bar{\hat{u}}_h$ within $\mathcal{F}_h^k$, facilitating the unique definition of a corresponding CR element by the CR lifting operator $\mathcal{L}_h^{\mathcal{CR}}$.

With these preparations, we present the following findings, detailing the connection between the L^2 norm of u_h and that of the function derived from $\mathcal{L}_h^{\mathcal{CR}}(\bar{\hat{u}}_h)$, along with the jump terms existing on the faces.

Proposition 3.4. Let $(u_h, \hat{u}_h) \in \mathcal{X}_h^k$. Then the following local inequality holds in each element K:

$$\|u_h\|^2_{L^2(\Omega;K)} \lesssim h_K^2|u_h|^2_{H^1(\Omega;K)} + h_K\|u_h - \hat{u}_h\|^2_{L^2(\Omega;\partial K)} + \left\|\mathcal{L}_h^{\mathcal{CR}}(\bar{\hat{u}}_h)\right\|^2_{L^2(\Omega;K)}, \tag{3.11}$$

and the global inequality will naturally hold as well:

$$\|u_h\|^2_{L^2(\Omega;\mathcal{T}_h)} \lesssim h_K^2|u_h|^2_{H^1(\Omega;\mathcal{T}_h)} + h_K\|u_h - \hat{u}_h\|^2_{L^2(\Omega;\partial\mathcal{T}_h)} + \left\|\mathcal{L}_h^{\mathcal{CR}}(\bar{\hat{u}}_h)\right\|^2_{L^2(\Omega;\mathcal{T}_h)} \tag{3.12}$$

Proof. We start by restricting our scope in an element K. In each K, we can split $\|u_h\|_{L^2(\Omega;K)}$ into two parts as

$$\|u_h\|_{L^2(\Omega;K)} \lesssim \|u_h - \bar{u}_{h,\partial K}\|_{L^2(\Omega;K)} + \|\bar{u}_{h,\partial K}\|_{L^2(\Omega;K)}. \tag{3.13}$$

where

$$\bar{u}_{h,\partial K} := \frac{1}{|\partial K|}\int_{\partial K} u_h\,ds \tag{3.14}$$

is defined as the average of u_h over ∂K. Using the Poincaré inequality in a single simplex (Lemma 2.6), the first quantity on the right-hand side of (3.13) can be controlled as:

$$\|u_h - \bar{u}_{h,\partial K}\|_{L^2(\Omega;K)} \lesssim h_K\|\nabla_h u_h\|_{L^2(\Omega;K)} \tag{3.15}$$

For the second quantity, since $u_{\partial K}$ is a constant, we have

$$\|\bar{u}_{h,\partial K}\|^2_{L^2(\Omega;K)} = |K|\,\bar{u}^2_{h,\partial K}.$$

This leads us to the objective of estimating $\bar{u}_{h,\partial K}$ to effectively bound $\|u_h\|_{L^2(\Omega;K)}$. By revisiting its definition, we can reinterpret this as the cumulative sum of integrals of u_h across the different faces e_i of element K, yielding the subsequent formulation:

$$\begin{aligned}\bar{u}_{h,\partial K} &= \frac{1}{|\partial K|}\int_{\partial K} u_h\,ds = \frac{1}{|\partial K|}\sum_{i=1}^{d+1}\int_{e_i} u_h\,ds\\ &= \frac{1}{|\partial K|}\sum_{i=1}^{d+1}\int_{e_i}(u_h - \bar{\hat{u}}_{h,e_i})\,ds + \frac{1}{|\partial K|}\sum_{i=1}^{d+1}\int_{e_i}\bar{\hat{u}}_{h,e_i}\,ds\end{aligned}$$

where definition of $\bar{\hat{u}}_{h,e_i}$ follows from (3.9). As $\int_{e_i}\bar{\hat{u}}_{h,e_i}\,ds = \int_{e_i}\hat{u}_h\,ds$, $\bar{u}_{h,\partial K}$ can be written as:

$$\bar{u}_{h,\partial K} = \frac{1}{|\partial K|}\int_{\partial K}(u_h - \hat{u}_h)\,ds + \frac{1}{|\partial K|}\sum_{i=1}^{d+1}\int_{e_i}\bar{\hat{u}}_{h,e_i}\,ds.$$

Applying the Cauchy-Schwarz inequality along with the assumption of shape regularity enables us to perform the following calculation:

$$\begin{aligned}(\bar{u}_{h,\partial K})^2 &\lesssim \frac{1}{|\partial K|^2}\left[\int_{\partial K}(u_h - \hat{u}_h)\,dx\right]^2 + \frac{1}{|\partial K|^2}\left[\sum_{i=1}^{d+1}\int_{e_i}\bar{\hat{u}}_{h,e_i}\,dx\right]^2\\ &\le \frac{1}{|\partial K|}\int_{\partial K}(u_h - \hat{u}_h)^2\,dx + \frac{1}{|\partial K|^2}\left(\sum_{i=1}^{d+1}|e_i|\,\bar{\hat{u}}_{h,e_i}\right)^2\\ &\lesssim \frac{1}{|\partial K|}\|u_h - \hat{u}_h\|^2_{L^2(\Omega;\partial K)} + \frac{1}{|\partial K|^2}\left(\sum_{i=1}^{d+1}|e_i|^2\right)\left(\sum_{i=1}^{d+1}\bar{\hat{u}}^2_{h,e_i}\right)\\ &\lesssim \frac{1}{|\partial K|}\|u_h - \hat{u}_h\|^2_{L^2(\Omega;\partial K)} + \sum_{i=1}^{d+1}(\bar{\hat{u}}_{h,e_i})^2\end{aligned}\tag{3.16}$$

Hence, using the principle of shape regularity once more, we obtain:

$$\|\bar{u}_{h,\partial K}\|^2_{L^2(\Omega,K)} = |K|\,u^2_{\partial K} \lesssim h_K\|u_h - \hat{u}_h\|^2_{L^2(\Omega;\partial K)} + h_K\|\bar{\hat{u}}_h\|^2_{L^2(\Omega;\partial K)},\tag{3.17}$$

where $\bar{\hat{u}}_h$ is defined in (3.10). Additionally, we have used the following fact to deduce (3.17)

$$\|\bar{\hat{u}}_h\|^2_{L^2(\Omega;\partial K)} = \sum_{i=1}^{d+1}|e_i|\;\bar{\hat{u}}^2_{h,e_i}$$

since $\bar{\hat{u}}_{h,e_i}$ is a constant for each i.

Then we use the lifting operator $\mathcal{L}_h^{\mathcal{CR}}$ to define a function $\mathcal{L}_h^{\mathcal{CR}}(\bar{\hat{u}}_h)$ in $\mathcal{CR}(\Omega;\mathcal{T}_h)$. According to Lemma 3.3, we get that in each element K,

$$\|\bar{\hat{u}}_h\|^2_{L^2(\Omega;\partial K)} \le \left\|\mathcal{L}_h^{\mathcal{CR}}(\bar{\hat{u}}_h)\right\|^2_{L^2(\Omega;\partial K)}\tag{3.18}$$

Now combining (3.18) with Lemma 2.3 (discrete trace inequality in simplex), we can rewrite (3.17) as

$$\begin{aligned}\|\bar{u}_{h,\partial K}\|^2_{L^2(\Omega,K)} &\lesssim h_K\|u_h - \hat{u}_h\|^2_{L^2(\Omega;\partial K)} + h_K\|\bar{\hat{u}}_h\|^2_{L^2(\Omega;\partial K)}\\ &\le h_K\|u_h - \hat{u}_h\|^2_{L^2(\Omega;\partial K)} + h_K\left\|\mathcal{L}_h^{\mathcal{CR}}(\bar{\hat{u}}_h)\right\|^2_{L^2(\Omega;\partial K)}\\ &\lesssim h_K\|u_h - \hat{u}_h\|^2_{L^2(\Omega;\partial K)} + \left\|\mathcal{L}_h^{\mathcal{CR}}(\bar{\hat{u}}_h)\right\|^2_{L^2(\Omega;K)}\end{aligned}\tag{3.19}$$

By inserting the estimates from (3.19) and (3.15) into (3.13), we get (3.11). And then summing the results over all elements K in $\mathcal{T}_h$, (3.12) follows.

□

In this analysis, we encounter the term $\left\|\mathcal{L}_h^{\mathcal{CR}}(\bar{\hat{u}}_h)\right\|^2_{L^2(\Omega;K)}$. This is where the Poincaré inequality for nonconforming spaces with no jump term, as outlined in Corollary 3.2, becomes relevant because this is a CR element. Consequently, an integral involving $\mathcal{L}_h^{\mathcal{CR}}(\bar{\hat{u}}_h)$ could emerge. To express this term in a form more consistent with the classical Poincaré inequality, we examine the difference between $\int_\Omega \mathcal{L}_h^{\mathcal{CR}}(\bar{\hat{u}}_h)\,dx$ and $\int_\Omega u_h\,dx$, leading to the subsequent finding:

Lemma 3.5. The difference between integral of $\mathcal{L}_h^{\mathcal{CR}}(\bar{\hat{u}}_h)$ and u_h can be controlled as

$$\left(\int_\Omega \mathcal{L}_h^{\mathcal{CR}}(\bar{\hat{u}}_h)\,dx\right)^2 \lesssim (h_K)^2|u_h|^2_{H^1(\Omega;\mathcal{T}_h)} + h_K\|u_h-\hat{u}_h\|^2_{L^2(\Omega;\partial\mathcal{T}_h)} + \left(\int_\Omega u_h\,dx\right)^2. \tag{3.20}$$

Proof. For simplicity of notation, we use ω_h to denote the piecewise linear function $\mathcal{L}_h^{\mathcal{CR}}(\bar{\hat{u}}_h)$ in the sense that $\omega_h|_K = \mathcal{L}_h^{\mathcal{CR}}(\bar{\hat{u}}_h)|_K$. Then

$$\begin{aligned}\int_\Omega \mathcal{L}_h^{\mathcal{CR}}(\bar{\hat{u}}_h)\,dx - \int_\Omega u_h\,dx &= \int_\Omega \omega_h\,dx - \int_\Omega u_h\,dx\\ &= \sum_{K\in\mathcal{T}_h}\int_K (\omega_h - u_h)\;dx = \sum_{K\in\mathcal{T}_h}\int_K (\bar{\omega}_{h,K} - \bar{u}_{h,K})\;dx\end{aligned}$$

where $\bar{\omega}_{h,K}$ and $\bar{u}_{h,K}$ denotes their averages over the simplex K. Since ω_h is a linear function, $\bar{\omega}_{h,K}$ can be evaluated via its value on the vertices and so we can compute that

$$\bar{\omega}_{h,K} = \frac{1}{d+1}\sum_{i=1}^{d+1}\bar{\hat{u}}_{h,e_i} \tag{3.21}$$

With this, we have

$$\begin{aligned}\int_\Omega \mathcal{L}_h^{\mathcal{CR}}(\bar{\hat{u}}_h)\,dx - \int_\Omega u_h\,dx &= \frac{1}{d+1}\sum_{K\in\mathcal{T}_h}\sum_{i=1}^{d+1}\int_K \left(\bar{\hat{u}}_{h,e_i} - \bar{u}_{h,K}\right)\;dx\\ &= \frac{1}{d+1}\sum_{K\in\mathcal{T}_h}\sum_{i=1}^{d+1}\left[\int_K \left(\bar{\hat{u}}_{h,e_i} - \bar{u}_{h,e_i}\right)\;dx + \int_K (\bar{u}_{h,e_i} - \bar{u}_{h,K})\;dx\right]\\ &= \frac{|K|}{d+1}\sum_{K\in\mathcal{T}_h}\sum_{i=1}^{d+1}\frac{1}{|e_i|}\int_{e_i}(\hat{u}_h - u_h)\;ds + \frac{1}{d+1}\sum_{K\in\mathcal{T}_h}\sum_{i=1}^{d+1}\int_K (\bar{u}_{h,e_i} - \bar{u}_{h,K})\;dx\\ &:= I_1 + I_2\end{aligned}$$

where $\bar{u}_{h,e_i}$, following the definition introduced in Lemma 2.6, is defined as average of $u_h|_K$ on the side e_i with the simplex K,

$$\bar{u}_{h,e_i} = \frac{1}{|e_i|}\int_{e_i} u_h|_K\;ds.$$

Therefore, we can control I_1, using the shape-regularity assumption and Cauchy-Schwarz inequality, as

$$\begin{aligned}(I_1)^2 = \frac{|K|^2}{(d+1)^2}\left[\sum_{K\in\mathcal{T}_h}\sum_{i=1}^{d+1}\frac{1}{|e_i|}\int_{e_i}(\hat{u}_h - u_h)\;ds\right]^2 &\lesssim \frac{|K|^2}{|\partial K|^2}\left[\sum_{K\in\mathcal{T}_h}\int_{\partial K}|\hat{u}_h - u_h|\;ds\right]^2\\ &\lesssim \frac{|K|}{|\partial K|^2}\left[\sum_{K\in\mathcal{T}_h}\left(\int_{\partial K}|\hat{u}_h - u_h|\;ds\right)^2\right]\\ &\lesssim \frac{|K|}{|\partial K|}\sum_{K\in\mathcal{T}_h}\int_{\partial K}|\hat{u}_h - u_h|^2\;ds\\ &\lesssim h_K\|u_h - \hat{u}_h\|^2_{L^2(\Omega;\partial\mathcal{T}_h)}\end{aligned}$$

while I_2 can be controlled using (2.11) from Lemma 2.6 as

$$\begin{aligned}(I_2)^2 = \frac{1}{(d+1)^2}\left[\sum_{K\in\mathcal{T}_h}\sum_{i=1}^{d+1}\int_K (\bar{u}_{h,e_i} - \bar{u}_{h,K})\;dx\right]^2 &\lesssim \frac{1}{|K|}\sum_{K\in\mathcal{T}_h}\left[\int_K |\bar{u}_{h,e_i} - \bar{u}_{h,K}|\;dx\right]^2\\ &\lesssim \sum_{K\in\mathcal{T}_h}\int_K |\bar{u}_{h,e_i} - \bar{u}_{h,K}|^2\;dx\\ &\lesssim (h_K)^2\sum_{K\in\mathcal{T}_h}\|\nabla_h u_h\|^2_{L^2(\Omega;K)}\\ &= (h_K)^2|u_h|^2_{H^1(\Omega;\mathcal{T}_h)}\end{aligned}$$

Combining the estimate for I_1 and I_2, we get

$$\left(\int_\Omega \mathcal{L}_h^{\mathcal{CR}}(\bar{\hat{u}}_h)\,dx\right)^2 \lesssim \left(\int_\Omega \mathcal{L}_h^{\mathcal{CR}}(\bar{\hat{u}}_h)\,dx - \int_\Omega u_h\,dx\right)^2 + \left(\int_\Omega u_h\,dx\right)^2$$
$$\lesssim (h_K)^2|u_h|^2_{H^1(\Omega;\mathcal{T}_h)} + h_K\|u_h - \hat{u}_h\|^2_{L^2(\Omega;\partial\mathcal{T}_h)} + \left(\int_\Omega u_h\,dx\right)^2.$$

Here we finish the proof. □

Now we state the main result of this section.

Theorem 3.6. Let $(u_h, \hat{u}_h) \in \mathcal{X}_h^k$. Then the following Poincaré inequalities hold:

(3.22)

$$\|u_h\|^2_{L^2(\Omega;\mathcal{T}_h)} \lesssim (h_K)^2|u_h|^2_{H^1(\Omega;\mathcal{T}_h)} + h_K\|u_h - \hat{u}_h\|^2_{L^2(\Omega;\partial\mathcal{T}_h)} + \left|\mathcal{L}_h^{\mathcal{CR}}(\bar{\hat{u}}_h)\right|^2_{H^1(\Omega;\mathcal{T}_h)} + \left(\int_\Omega \mathcal{L}_h^{\mathcal{CR}}(\bar{\hat{u}}_h)\,dx\right)^2$$

and

$$\|u_h\|^2_{L^2(\Omega;\mathcal{T}_h)} \lesssim (h_K)^2|u_h|^2_{H^1(\Omega;\mathcal{T}_h)} + h_K\|u_h - \hat{u}_h\|^2_{L^2(\Omega;\partial\mathcal{T}_h)} + \left|\mathcal{L}_h^{\mathcal{CR}}(\bar{\hat{u}}_h)\right|^2_{H^1(\Omega;\mathcal{T}_h)} + \left(\int_\Gamma \hat{u}_h\,ds\right)^2 \tag{3.23}$$

where Γ is combination of boundary faces that has a positive measure, namely, $\Gamma = \bigcup_{i=1}^N e_i$ such that $e_i \in \partial\mathcal{T}_h^b$ and $\{e_1, e_2, \cdots, e_N\}$ are different faces. In addition, the following variant of (3.22) expressing in term of integral of u_h also holds:

$$\|u_h\|^2_{L^2(\Omega;\mathcal{T}_h)} \lesssim (h_K)^2|u_h|^2_{H^1(\Omega;\mathcal{T}_h)} + h_K\|u_h - \hat{u}_h\|^2_{L^2(\Omega;\partial\mathcal{T}_h)} + \left|\mathcal{L}_h^{\mathcal{CR}}(\bar{\hat{u}}_h)\right|^2_{H^1(\Omega;\mathcal{T}_h)} + \left(\int_\Omega u_h\,dx\right)^2 \tag{3.24}$$

Proof. As $\mathcal{L}_h^{\mathcal{CR}}(\bar{\hat{u}}_h) \in \mathcal{CR}(\Omega;\mathcal{T}_h)$, estimate (3.4) and (3.5) in Corollary 3.2 hold for $\mathcal{L}_h^{\mathcal{CR}}(\bar{\hat{u}}_h)$. Combining (3.4) with Proposition 3.4, (3.22) will be immediately obtained. Similarly, combining (3.5) with Proposition 3.4 will lead to

$$\|u_h\|^2_{L^2(\Omega;\mathcal{T}_h)} \lesssim h_K^2|u_h|^2_{H^1(\Omega;\mathcal{T}_h)} + h_K\|u_h - \hat{u}_h\|^2_{L^2(\Omega;\partial\mathcal{T}_h)} + \left|\mathcal{L}_h^{\mathcal{CR}}(\bar{\hat{u}}_h)\right|^2_{H^1(\Omega;\mathcal{T}_h)} + \left(\int_\Gamma \mathcal{L}_h^{\mathcal{CR}}(\bar{\hat{u}}_h)\,ds\right)^2$$

Since Γ is a combination of boundary faces, we have

$$\int_\Gamma \mathcal{L}_h^{\mathcal{CR}}(\bar{\hat{u}}_h)\,ds = \int_{\bigcup_{i=1}^N e_i} \mathcal{L}_h^{\mathcal{CR}}(\bar{\hat{u}}_h)\,ds$$
$$= \sum_{i=1}^N \int_{e_i} \mathcal{L}_h^{\mathcal{CR}}(\bar{\hat{u}}_h)\,ds = \sum_{i=1}^N \int_{e_i} \bar{\hat{u}}_h\,ds = \sum_{i=1}^N \int_{e_i} \hat{u}_h\,ds = \int_\Gamma \hat{u}_h\,ds$$

and so (3.23) is obtained.

To the end, (3.22) together with Lemma 3.5 will immediately lead to (3.24). □

4. Discrete Trace Inequality

In this section, we present an analogue of the trace theorem specifically designed for hybridizable spaces, which is an essential tool for analyzing boundary value problems. We want to highlight the difference between the notations $H^1(\Omega)$ and $L^2(\Omega)$—indicating the standard Sobolev space and the square integrable space, respectively—and the specialized notations $H^1(\Omega;\mathcal{T}_h)$ and $L^2(\Omega;\mathcal{T}_h)$. Our discussion commences with a finding from [7] that provides insight into $H^1(\Omega;\mathcal{T}_h)$, laying the groundwork for understanding this space through its relationship with functions belonging to $H^1(\Omega)$.

Lemma 4.1. Let $f \in H^1(\Omega;\mathcal{T}_h)$. Then there exists a function $\zeta \in H^1(\Omega)$ such that

$$\begin{aligned}\|\nabla\zeta\|^2_{L^2(\Omega)} + \frac{1}{h_K}\|f-\zeta\|^2_{L^2(\partial\Omega)} + \frac{1}{(h_K)^2}\|f-\zeta\|^2_{L^2(\Omega)} \\ \lesssim |f|^2_{H^1(\Omega;\mathcal{T}_h)} + \sum_{e\in\partial\mathcal{T}_h^i}\frac{1}{|e|}\,\|\Pi_{0,e}[[f]]_e\|^2_{L^2(\Omega;e)}\end{aligned} \tag{4.1}$$

where $\Pi_{0,e}$ is the orthogonal projection operator from $L^2(\Omega;e)$ onto $\mathcal{P}^0(\Omega;e)$, the space of constant functions on e.

Proof. See [7, Proposition 2.7]. □

We observe that the jump term appears again in the inequality, similar to the discrete Poincaré inequality for classical non-conforming elements discussed in Section 3.1. This observation leads us to concentrate on functions from the CR space $\mathcal{CR}(\Omega;\mathcal{T}_h)$, where the jump term is eliminated. Consequently, we obtain the following result:

Lemma 4.2. Let $\omega_h \in \mathcal{CR}(\Omega;\mathcal{T}_h)$, then the following estimates hold:

$$\|\omega_h\|^2_{L^2(\Omega;\partial\mathcal{T}_h^b)} \lesssim \left[1+(h_K)^2\right]|\omega_h|^2_{H^1(\Omega;\mathcal{T}_h)} + \left(\int_\Omega \omega_h\,dx\right)^2 \tag{4.2}$$

and

$$\|\omega_h\|^2_{L^2(\Omega;\partial\mathcal{T}_h^b)} \lesssim (1+h_K)|\omega_h|^2_{H^1(\Omega;\mathcal{T}_h)} + \left(\int_\Gamma \omega_h\,ds\right)^2 \tag{4.3}$$

where Γ is combination of boundary faces that has a positive measure, namely, $\Gamma = \bigcup_{i=1}^N e_i$ such that $e_i \in \partial\mathcal{T}_h^b$ and $\{e_1, e_2, \cdots, e_N\}$ are different boundary faces.

Proof. For a given $\omega_h \in \mathcal{CR}(\Omega;\mathcal{T}_h)$ and based on Lemma 4.1, there exists a function $\zeta \in H^1(\Omega)$ satisfying the relationship described in (4.1),

$$\|\nabla\zeta\|^2_{L^2(\Omega)} + \frac{1}{h_K}\|\omega_h-\zeta\|^2_{L^2(\partial\Omega)} + \frac{1}{(h_K)^2}\|\omega_h-\zeta\|^2_{L^2(\Omega)} \lesssim |\omega_h|^2_{H^1(\Omega;\mathcal{T}_h)} \tag{4.4}$$

as every interior face satisfies,

$$\int_e [[\omega_h]]_e\,ds = 0.$$

Next, by decomposing ω_h into $(\omega_h-\zeta)$ and ζ, we can derive an estimate for the trace of ω_h on $\partial\mathcal{T}_h^b$ as follows:

$$\|\omega_h\|^2_{L^2(\Omega;\partial\mathcal{T}_h^b)} \lesssim \|\omega_h-\zeta\|^2_{L^2(\Omega;\partial\mathcal{T}_h^b)} + \|\zeta\|^2_{L^2(\Omega;\partial\mathcal{T}_h^b)} \tag{4.5}$$

The first part has already appeared in (4.4). Regarding the second portion, given that $\zeta \in H^1(\Omega)$, the classical trace theorem and Poincaré inequality related to the mean-value are applicable, resulting in:

$$\begin{aligned}\|\zeta\|^2_{L^2(\Omega;\partial\mathcal{T}_h^b)} &\lesssim \|\nabla\zeta\|^2_{L^2(\Omega)} + \left(\int_\Omega \zeta\,dx\right)^2 \\ &\lesssim \|\nabla\zeta\|^2_{L^2(\Omega)} + \left[\int_\Omega(\zeta-\omega_h)\,dx\right]^2 + \left(\int_\Omega \omega_h\,dx\right)^2 \\ &\lesssim \|\nabla\zeta\|^2_{L^2(\Omega)} + \|\omega_h-\zeta\|^2_{L^2(\Omega;\mathcal{T}_h)} + \left(\int_\Omega \omega_h\,dx\right)^2.\end{aligned}$$

The last line is deduced through employing the Cauchy-Schwarz inequality and acknowledging Ω's finite measure. Analogously, applying a Poincaré inequality relative to the boundary mean value provides:

$$\begin{aligned}\|\zeta\|^2_{L^2(\Omega;\partial\mathcal{T}_h^b)} &\lesssim \|\nabla\zeta\|^2_{L^2(\Omega)} + \left(\int_\Gamma \zeta\, ds\right)^2 \\ &\lesssim \|\nabla\zeta\|^2_{L^2(\Omega)} + \left[\int_{\partial\Omega}(\zeta-\omega_h)\, ds\right]^2 + \left(\int_\Gamma \omega_h\, ds\right)^2 \\ &\lesssim \|\nabla\zeta\|^2_{L^2(\Omega)} + \|\omega_h-\zeta\|^2_{L^2(\Omega;\partial\mathcal{T}_h^b)} + \left(\int_\Gamma \omega_h\, ds\right)^2,\end{aligned}$$

due to Γ's finite measure. Integrating these findings into (4.5) and associating it with (4.4) leads to:

$$\begin{aligned}\|\omega_h\|^2_{L^2(\Omega;\partial\mathcal{T}_h^b)} &\lesssim \|\nabla\zeta\|^2_{L^2(\Omega)} + \|\omega_h-\zeta\|^2_{L^2(\Omega;\partial\mathcal{T}_h^b)} + \|\omega_h-\zeta\|^2_{L^2(\Omega;\mathcal{T}_h)} + \left(\int_\Omega \omega_h\, dx\right)^2 \\ &\lesssim \left[1+h_K+(h_K)^2\right]|\omega_h|^2_{H^1(\Omega;\mathcal{T}_h)} + \left(\int_\Omega \omega_h\, dx\right)^2 \\ &\lesssim \left[1+(h_K)^2\right]|\omega_h|^2_{H^1(\Omega;\mathcal{T}_h)} + \left(\int_\Omega \omega_h\, dx\right)^2,\end{aligned}$$

and

$$\begin{aligned}\|\omega_h\|^2_{L^2(\Omega;\partial\mathcal{T}_h^b)} &\lesssim \|\nabla\zeta\|^2_{L^2(\Omega)} + \|\omega_h-\zeta\|^2_{L^2(\Omega;\partial\mathcal{T}_h)} + \left(\int_\Gamma \omega_h\, ds\right)^2 \\ &\lesssim (1+h_K)|\omega_h|^2_{H^1(\Omega;\mathcal{T}_h)} + \left(\int_\Gamma \omega_h\, ds\right)^2.\end{aligned}$$

We here yield the anticipated outcomes.

□

Remark 4.3. This finding indicates that when the average value of a CR element on the boundary can be evaluated, the classical trace theorem from the H^1 Sobolev space can be extended to the non-conforming CR space.

With this insight, we now shift our focus to formulating a trace argument for hybridizable spaces, employing a methodology akin to that used in proving the Poincaré inequality. Our goal is to establish a bridge between u_h and $\hat{u}_h$ by examining the discrepancies between their average values and their individual values, and subsequently mapping these boundary averages into CR spaces. This process leads to the following theorem:

Theorem 4.4. Let $(u_h,\hat{u}_h)\in\mathcal{X}_h^k$, then the following trace inequalities hold:

$$\|u_h\|^2_{L^2(\Omega;\partial\mathcal{T}_h^b)} \lesssim h_K|u_h|^2_{H^1(\Omega;\mathcal{T}_h)} + \|u_h-\hat{u}_h\|^2_{L^2(\Omega;\partial\mathcal{T}_h^b)} + (1+h_K)|\mathcal{L}_h^{\mathcal{CR}}(\bar{\hat{u}}_h)|^2_{H^1(\Omega;\mathcal{T}_h)} + \left(\int_\Gamma \hat{u}_h\, ds\right)^2 \tag{4.6}$$

and

$$\|\hat{u}_h\|^2_{L^2(\Omega;\partial\mathcal{T}_h^b)} \lesssim h_K|u_h|^2_{H^1(\Omega;\mathcal{T}_h)} + \|u_h-\hat{u}_h\|^2_{L^2(\Omega;\partial\mathcal{T}_h^b)} + (1+h_K)|\mathcal{L}_h^{\mathcal{CR}}(\bar{\hat{u}}_h)|^2_{H^1(\Omega;\mathcal{T}_h)} + \left(\int_\Gamma \hat{u}_h\, ds\right)^2. \tag{4.7}$$

Here Γ has the same definition as Lemma 4.2.

Proof. We evaluate the estimate for $\|u_h\|_{L^2(\Omega;\partial\mathcal{T}_h^b)}$. This norm is derived from the trace of u_h on $\partial\mathcal{T}_h^b$. By the definition of $\partial\mathcal{T}_h^b$, the boundary of the mesh can be expressed as $\partial\mathcal{T}_h^b=\bigcup_{i=1}^{N_{h_K}} e_i$ for a given mesh with h_K as its mesh diameter, where $\partial\mathcal{T}_h^b$ consists of N_{h_K} distinct faces. Therefore, we can state:

$$\|u_h\|^2_{L^2(\Omega;\partial\mathcal{T}_h^b)} = \sum_{i=1}^{N_{h_K}} \|u_h\|^2_{L^2(\Omega;e_i)}$$

For each boundary face e_i, if we consider K_i to be the element it belongs to, we can decompose u_h into two parts and achieve:

$$\|u_h\|^2_{L^2(\Omega;e_i)} \lesssim \|u_h - \bar{u}_{h,e_i}\|^2_{L^2(\Omega;e_i)} + \|\bar{u}_{h,e_i}\|^2_{L^2(\Omega;e_i)} \tag{4.8}$$

where $\bar{u}_{h,e_i}$ is the average value of u_h on face e_i, defined by:

$$\bar{u}_{h,e_i} = \frac{1}{|e_i|}\int_{e_i} u_h\, ds$$

For the first term, utilizing Lemma 2.3 and Lemma 2.6, which are the discrete trace inequality and discrete Poincaré inequality in a simplex, we can establish bound as follows:

$$\|u_h - \bar{u}_{h,e_i}\|^2_{L^2(\Omega;e_i)} \lesssim \frac{1}{h_K}\|u_h - \bar{u}_{h,e_i}\|^2_{L^2(\Omega;K_i)} \lesssim h_K\|\nabla u_h\|^2_{L^2(\Omega;K_i)}, \tag{4.9}$$

Given that $\bar{u}_{h,e_i}$ is a constant, we can estimate the second term as follows:

$$\begin{aligned}
(\bar{u}_{h,e_i})^2 &= \frac{1}{|e_i|^2}\left(\int_{e_i} u_h\, ds\right)^2 \\
&\lesssim \frac{1}{|e_i|^2}\left[\int_{e_i}(u_h - \hat{u}_h)\, ds\right]^2 + \frac{1}{|e_i|^2}\left(\int_{e_i}\hat{u}_h\, ds\right)^2 \\
&\lesssim \frac{1}{|e_i|}\|u_h - \hat{u}_h\|^2_{L^2(\Omega;e_i)} + (\bar{\hat{u}}_{h,e_i})^2,
\end{aligned}$$

where $\bar{\hat{u}}_{h,e_i}$ is detailed in (3.9). Consequently,

$$\|\bar{u}_{h,e_i}\|^2_{L^2(\Omega;e_i)} = |e_i|(\bar{u}_{h,e_i})^2 \lesssim \|u_h - \hat{u}_h\|^2_{L^2(\Omega;e_i)} + \|\bar{\hat{u}}_{h,e_i}\|^2_{L^2(\Omega;e_i)}.$$

Following Lemma 3.3 and especially, estimate (3.8), it's evident that:

$$\|\bar{u}_{h,e_i}\|^2_{L^2(\Omega;e_i)} \lesssim \|u_h - \hat{u}_h\|^2_{L^2(\Omega;e_i)} + \|\mathcal{L}_h^{\mathcal{CR}}(\bar{\hat{u}}_h)\|^2_{L^2(\Omega;e_i)},$$

with $\bar{\hat{u}}_h$ specified in (3.10). Merging these results leads to:

$$\|u_h\|^2_{L^2(\Omega;e_i)} \lesssim h_K\|\nabla u_h\|^2_{L^2(\Omega;K_i)} + \|u_h - \hat{u}_h\|^2_{L^2(\Omega;e_i)} + \|\mathcal{L}_h^{\mathcal{CR}}(\bar{\hat{u}}_h)\|^2_{L^2(\Omega;e_i)} \tag{4.10}$$

Summarizing these results gives:

$$\|u_h\|^2_{L^2(\Omega;\partial\mathcal{T}_h^b)} = \sum_{i=1}^{N_h}\|u_h\|^2_{L^2(\Omega;e_i)} \lesssim h_K|u_h|^2_{H^1(\Omega;\mathcal{T}_h)} + \|u_h - \hat{u}_h\|^2_{L^2(\Omega;\partial\mathcal{T}_h^b)} + \|\mathcal{L}_h^{\mathcal{CR}}(\bar{\hat{u}}_h)\|^2_{L^2(\Omega;\partial\mathcal{T}_h^b)} \tag{4.11}$$

By (4.3) from Lemma 4.2 and the definition of CR lifting operator, the trace of $\mathcal{L}_h^{\mathcal{CR}}(\bar{\hat{u}}_h)$ can be bounded as

$$\begin{aligned}
\|\mathcal{L}_h^{\mathcal{CR}}(\bar{\hat{u}}_h)\|^2_{L^2(\Omega;\partial\mathcal{T}_h^b)} &\lesssim (1+h_K)|\mathcal{L}_h^{\mathcal{CR}}(\bar{\hat{u}}_{h,e})|^2_{H^1(\Omega;\mathcal{T}_h)} + \left(\int_\Gamma \mathcal{L}_h^{\mathcal{CR}}(\bar{\hat{u}}_h)\, ds\right)^2 \\
&= (1+h_K)|\mathcal{L}_h^{\mathcal{CR}}(\bar{\hat{u}}_{h,e})|^2_{H^1(\Omega;\mathcal{T}_h)} + \left(\int_\Gamma \bar{\hat{u}}_h\, ds\right)^2 \\
&= (1+h_K)|\mathcal{L}_h^{\mathcal{CR}}(\bar{\hat{u}}_{h,e})|^2_{H^1(\Omega;\mathcal{T}_h)} + \left(\int_\Gamma \hat{u}_h\, ds\right)^2
\end{aligned} \tag{4.12}$$

Inserting (4.9), (4.11) and (4.12) into (4.8), we have shown the estimate (4.6). To obtain (4.7), we simply need to notice the fact that

$$\|\hat{u}_h\|^2_{L^2(\Omega;\partial\mathcal{T}_h^b)} \lesssim \|u_h\|^2_{L^2(\Omega;\partial\mathcal{T}_h^b)} + \|\hat{u}_h - u_h\|^2_{L^2(\Omega;\partial\mathcal{T}_h^b)}$$

and then the desired result follows. □

Remark 4.5. In the estimates (4.6) and (4.7), the term $\left(\int_\Gamma \hat{u}_h\, ds\right)^2$ can be replaced with $\left(\int_\Gamma u_h\, ds\right)^2$. This adjustment is viable as the term $\|\hat{u}_h - u_h\|^2_{L^2(\Omega;\partial\mathcal{T}_h^b)}$ is involved in the estimate. Moreover, it's also practical to exchange this term with the integral of $\mathcal{L}_h^{\mathcal{CR}}(\bar{\hat{u}}_h)$ over the entire domain Ω, opting for (4.2) over (4.3) to establish the trace estimate for $\|\mathcal{L}_h^{\mathcal{CR}}(\bar{\hat{u}}_h)\|^2_{L^2(\Omega;\partial\mathcal{T}_h^b)}$.

5. Application to HDG formulation

In this section, we will discuss how Poincaré inequalities and trace inequalities developed above can actually benefit in analysis for problems set up by HDG method. In particular, we will use these tools to obtain uniform energy estimates for the solutions for second-order elliptic equations in dependent of mesh size h_K with a minimal regularity assumption. For sake of simplicity, we will only consider Poisson equation as a model problem and the analysis can be extended to more general case of second-order elliptic equations easily.

5.1. **Boundary Lifting Operator.** As a start, we introduce the definition of a discrete gradient operator, which will be called a lifting operator in the following. This operator is designed to approximate the distributional gradient which is also a common methodology in analyzing discontinuous schemes presented in related works [11, 29, 48, 50, 51, 62, 63]. The cornerstone of this discrete gradient operator lies in a critical observation regarding the nature of functions within $\mathcal{X}_h^k$ [11]. Specifically, it is noted that these functions exhibit discontinuities, which in turn implies that their distributional gradient is influenced by the difference of u_h and $\hat{u}_h$ on the interfaces of elements.

In each element K, we introduce a local lifting operator $\mathcal{G}_h^{\partial K} : L^2(\Omega; \partial K) \to \boldsymbol{\mathcal{P}}^k(K)$, inspired by the previously discussed contents. This operator transforms a function $\hat{\mu}$, defined on ∂K, into a vector-valued piecewise polynomial function. Specifically, for each function $\hat{\mu} \in L^2(\Omega; \partial K)$, we define $\mathcal{G}_h^{\partial K}(\hat{\mu})$ as follows:

$$\int_K \mathcal{G}_h^{\partial K}(\hat{\mu}) \cdot \boldsymbol{\omega_h}\, dx = \int_{\partial K} \hat{\mu}\, \boldsymbol{\omega_h} \cdot \boldsymbol{n}\, ds \tag{5.1}$$

for any $\boldsymbol{\omega_h} \in \boldsymbol{\mathcal{P}}^k(K)$. The global lifting operator $\mathcal{G}_h^k : L^2(\Omega; \partial \mathcal{T}_h) \to \boldsymbol{\mathcal{V}}_h^k$ is then defined through the restriction to each element, such that $\mathcal{G}_h^k(\hat{\mu})|_K = \mathcal{G}_h^{\partial K}(\hat{\mu}|_K)$ for every $\hat{\mu} \in L^2(\Omega; \partial \mathcal{T}_h)$. Hence, it should comply with the form:

$$\int_\Omega \mathcal{G}_h^k(\hat{\mu}) \cdot \boldsymbol{\omega_h}\, dx = \sum_{K \in \mathcal{T}_h} \int_K \mathcal{G}_h^k(\hat{\mu}) \cdot \boldsymbol{\omega_h}\, dx = \sum_K \int_{\partial K} \hat{\mu}\, \boldsymbol{\omega_h} \cdot \boldsymbol{n}\, ds, \qquad \forall \boldsymbol{\omega_h} \in \boldsymbol{\mathcal{V}}_h^k. \tag{5.2}$$

The following lemma provides a local estimate for this lifting operator, emerging as a direct consequence of the discrete trace inequality Lemma 2.3.

Lemma 5.1. For every $\hat{\mu} \in L^2(\Omega; \partial K)$,

$$\|\mathcal{G}_h^{\partial K}(\hat{\mu})\|^2_{\boldsymbol{L}^2(\Omega;K)} \lesssim \frac{1}{h_K} \|\hat{\mu}\|^2_{L^2(\Omega;\partial K)}.$$

Proof. Let $\boldsymbol{\omega_h} = \mathcal{G}_h^{\partial K}(\hat{\mu})$ in equation (5.1), by Cauchy-Schwarz inequality we have

$$\|\mathcal{G}_h^{\partial K}(\hat{\mu})\|^2_{\boldsymbol{L}^2(\Omega;K)} = \int \hat{\mu}\, \mathcal{G}_h^{\partial K}(\hat{\mu}) \cdot \boldsymbol{n}\, ds \le \|\hat{\mu}\|_{L^2(\Omega;\partial K)} \|\mathcal{G}_h^{\partial K}(\hat{\mu}) \cdot \boldsymbol{n}\|_{L^2(\Omega;\partial K)}.$$

By Lemma 2.3, combining with Remark 2.4 and Remark 2.5, we can conclude that

$$\|\mathcal{G}_h^{\partial K}(\hat{\mu}) \cdot \boldsymbol{n}\|_{L^2(\Omega;\partial K)} \lesssim \frac{1}{h_K^{\frac{1}{2}}} \|\mathcal{G}_h^{\partial K}(\hat{\mu})\|_{L^2(\Omega;K)}.$$

Combining these two formulas and the claim of this lemma follows. ☐

This result can be extended to be an estimate for the global lifting operator by direct addition of the part in each element, which is summarized as follows.

Corollary 5.2. For $\hat{\mu} \in L^2(\Omega; \partial \mathcal{T}_h)$,

$$\|\mathcal{G}_h^k(\hat{\mu})\|^2_{\boldsymbol{L}^2(\Omega;\mathcal{T}_h)} \lesssim \frac{1}{h_K} \|\hat{\mu}\|^2_{L^2(\Omega;\partial \mathcal{T}_h)}.$$

5.2. **Problem Setup.** We will briefly outline the HDG method's formulation and structure for the Poisson problem, then explore how the Poincaré inequality and the trace inequality we derived can be used for stability analysis towards it. This contrasts with [46], where a translation argument was employed for deducing stability.

In this discussion, we address the Poisson equation with mixed boundary conditions as a model problem. Other types of boundary conditions can also be accommodated within this framework. The strong form of the Poisson equation in Ω is given by:

$$\begin{cases} -\Delta u = f & \text{in } \Omega, \\ u = u_D & \text{on } \Gamma_D, \\ \nabla u \cdot \boldsymbol{n} = u_N & \text{on } \Gamma_N. \end{cases} \tag{5.3}$$

Here, $\partial\Omega = \bar{\Gamma}_D \bigcup \bar{\Gamma}_N$ and $\Gamma_D \bigcap \Gamma_N = \emptyset$, with f serving as the source term.

A mixed formulation is introduced by defining $\boldsymbol{p} = -\nabla u$, allowing the system to be reformulated as:

$$\begin{cases} \nabla \cdot \boldsymbol{p} = f & \text{in } \Omega, \\ \boldsymbol{p} + \nabla u = 0 & \text{in } \Omega, \\ u = u_D & \text{on } \Gamma_D. \\ \boldsymbol{p} \cdot \boldsymbol{n} = -u_N & \text{on } \Gamma_N \end{cases} \tag{5.4}$$

In situations where the solution possesses sufficient regularity, these two formulations are equivalent. To solve this problem numerically, the domain is partitioned into a mesh $\mathcal{T}_h$, and we will continue employing the notations introduced in Section 2.1. Upon establishing a mesh, we adhere to the standard HDG formulation for second-order elliptic equations as documented in [21, 22, 25, 61] to devise the scheme. Specifically, within each element K, our objective is to find $(\boldsymbol{p}_h, u_h) \in \boldsymbol{\mathcal{V}}_h^k \times \mathcal{U}_h^k$ fulfilling:

$$(\boldsymbol{p}_h, \boldsymbol{q}_h)_K = (u_h, \nabla \cdot \boldsymbol{q}_h)_K - \langle \hat{u}_h, \boldsymbol{q}_h \cdot \boldsymbol{n} \rangle_{\partial K}, \tag{5.5}$$

and

$$-(\boldsymbol{p}_h, \nabla v_h)_K + \langle \hat{\boldsymbol{p}}_h \cdot \boldsymbol{n}, v \rangle_{\partial K} = (f, v)_K, \tag{5.6}$$

for every test function pair $(\boldsymbol{q}_h, v_h) \in \boldsymbol{\mathcal{V}}_h^k \times \mathcal{U}_h^k$. The Dirichlet boundary condition is imposed as [24]:

$$\langle \hat{u}_h, \hat{\mu} \rangle_{\Gamma_D} = \langle u_D, \hat{\mu} \rangle_{\Gamma_D}, \tag{5.7}$$

for all $\hat{\mu} \in \mathcal{F}_h^k$. Numerical traces of the fluxes in the HDG scheme are typically chosen as [22, 53, 54, 55, 56]:

$$\hat{\boldsymbol{p}}_h \cdot \boldsymbol{n} = \boldsymbol{p} \cdot \boldsymbol{n} + \tau(u_h - \hat{u}_h), \tag{5.8}$$

where τ is a stabilization function significantly affecting the scheme's effectiveness and accuracy. Numerous studies have been dedicated to this selection, for instance, [24, 25, 49] and references therein. It is noted that choosing τ as a constant on a simplicial mesh ensures optimal convergence order. However, selecting the stabilization function to be of order $O(\frac{1}{h_K})$ results in a loss of one convergence order in both the locally post-processed approximation to the scalar variable and the approximate to the gradient. Yet, conducting stability analysis for the constant case presents more challenges from a traditional standpoint. We aim to focus on this scenario using the newly developed tools above.

Once we have established the local problems, a global problem can be formulated to determine $\hat{u}_h$, considering the behavior of the numerical fluxes as outlined in [61]:

$$\langle \hat{\boldsymbol{p}}_h \cdot \boldsymbol{n}, \hat{\mu} \rangle_{\partial \mathcal{T}_h^i} + \langle \hat{\boldsymbol{p}}_h \cdot \boldsymbol{n}, \hat{\mu} \rangle_{\Gamma_N} = -\langle \hat{\mu}, u_N \rangle_{\Gamma_N} \tag{5.9}$$

This equation also implements the Neumann boundary.

Merging (5.5)-(5.9) leads to summarizing the HDG formulation as the following task: Finding $(\boldsymbol{p}_h, u_h, \hat{u}_h) \in \boldsymbol{\mathcal{V}}_h^k \times \mathcal{U}_h^k \times \mathcal{F}_h^k$ such that:

$$(\boldsymbol{p}_h, \boldsymbol{q}_h)_{\mathcal{T}_h} = (u_h, \nabla \cdot \boldsymbol{q}_h)_{\mathcal{T}_h} - \langle \hat{u}_h, \boldsymbol{q}_h \cdot \boldsymbol{n} \rangle_{\partial \mathcal{T}_h} \tag{5.10a}$$

$$\tau \langle u_h - v_h, \hat{u}_h - \hat{v}_h \rangle_{\partial \mathcal{T}_h} + (\nabla \cdot \boldsymbol{p}_h, v_h)_{\mathcal{T}_h} - \langle \boldsymbol{p}_h \cdot \boldsymbol{n}, \hat{v}_h \rangle_{\partial \mathcal{T}_h} = (f, v)_{\mathcal{T}_h} + \langle u_N, \hat{v}_h \rangle_{\Gamma_N} \tag{5.10b}$$

$$\langle \hat{u}_h, \hat{v}_h \rangle_{\Gamma_D} = \langle u_D, \hat{v}_h \rangle_{\Gamma_D} \tag{5.10c}$$

for all $(\boldsymbol{q}_h, v_h, \hat{v}_h) \in \boldsymbol{\mathcal{V}}_h^k \times \mathcal{U}_h^k \times \mathcal{F}_h^k$. For simplicity, τ will be assumed as a fixed positive constant throughout. In a more general context, τ could be regarded as a function defined over the skeleton with a positive lower bound. The ensuing analysis would remain applicable to such a scenario. It's also assumed, without loss of generality, that the mesh properly decomposes Γ_D and Γ_N, meaning each can be expressed as a union of non-disjoint boundary faces. The well-posedness of this scheme has been presented in several studies, such as [17]. The subsequent energy-type argument is standard and directly follows from the HDG scheme.

Lemma 5.3. The numerical solution $(\boldsymbol{p}_h, u_h, \hat{u}_h) \in \boldsymbol{\mathcal{V}}_h^k \times \mathcal{U}_h^k \times \mathcal{F}_h^k$, solving (5.10), satisfies:

$$\|\boldsymbol{p}_h\|^2_{\boldsymbol{L}^2(\Omega;\mathcal{T}_h)} + \tau \|u_h - \hat{u}_h\|^2_{L^2(\Omega;\partial\mathcal{T}_h)} = (f, u_h)_{\mathcal{T}_h} + \langle u_N, \hat{u}_h \rangle_{\Gamma_N}, \tag{5.11}$$

and

$$\|\hat{u}_h\|^2_{L^2(\Omega;\Gamma_D)} \le \|u_D\|^2_{L^2(\Omega;\Gamma_D)}. \tag{5.12}$$

Proof. By setting $\boldsymbol{q}_h = \boldsymbol{p}_h, v_h = u_h$, and $\hat{v}_h = \hat{u}_h$ in (5.10a) and (5.10b), equation (5.11) is obtained, whereas (5.12) follows from the Cauchy-Schwarz inequality by choosing $\hat{v}_h = \hat{u}_h$ in (5.10c). □

It's important to note that in the HDG scheme, energy estimation is conducted concerning $\boldsymbol{p}_h$, rather than $\nabla_h u_h$ or $\nabla \mathcal{L}_h^{\mathcal{CR}}(\bar{\hat{u}}_h)$. Consequently, the direct application of the analytical techniques we've previously discussed is not feasible without establishing a proper connection between $\boldsymbol{p}_h$ and these elements. Identifying this relationship will be the primary objective in the following discussions.

5.3. **Poincaré and Trace Inequalities for HDG.** Building on the previous discussion, our goal here is to elucidate the relationships between $\|u_h\|_{L^2(\Omega;\mathcal{T}_h)}$, $\|\hat{u}_h\|_{L^2(\Omega;\partial\mathcal{T}_h)}$, and $\|\boldsymbol{p}_h\|_{\boldsymbol{L}^2(\Omega;\mathcal{T}_h)}$, which are crucial to the analysis of HDG scheme. We recognize that (5.10a) uniquely defines $\boldsymbol{p}_h$ in terms of $(u_h, \hat{u}_h)$, serving as the bridge for us to link $\nabla_h u_h$ with $\boldsymbol{p}_h$, and similarly, to connect $\nabla_h \mathcal{L}_h^{\mathcal{CR}}(\bar{\hat{u}}_h)$ with $\boldsymbol{p}_h$. These connections will lay the groundwork for adapting the Poincaré and trace inequalities, previously established for hybridizable spaces, to the specific context of the HDG scheme.

We initiate our analysis by examining ∇u within each element K, which yields the subsequent result:

Lemma 5.4. Given $(u_h, \hat{u}_h) \in \mathcal{X}_h^k$, and assuming $\boldsymbol{p}_h$ satisfies (5.10a), then:

$$\|\nabla u_h\|^2_{L^2(\Omega;K)} \lesssim \|\boldsymbol{p}_h\|^2_{\boldsymbol{L}^2(\Omega;K)} + \frac{1}{h_K}\|u - \hat{u}_h\|^2_{L^2(\Omega;\partial K)}. \tag{5.13}$$

Proof. Using integration by parts, the equation (5.10a) can be reformulated as:

$$(\boldsymbol{p}_h, \boldsymbol{q}_h)_K = -(\nabla u_h, \boldsymbol{q}_h)_K + \langle u_h - \hat{u}_h, \boldsymbol{q}_h \cdot \boldsymbol{n} \rangle_{\partial K}.$$

Referring to the definition of the lifting operator in (5.1), we find an equivalent expression:

$$(\nabla u_h, \boldsymbol{q}_h)_K = (-\boldsymbol{p}_h + \mathcal{G}_h^{\partial K}(u_h - \hat{u}_h), \boldsymbol{q}_h)_K.$$

This holds true for all $\boldsymbol{q}_h \in \mathcal{P}^k(K)$. Given that $\nabla u, \boldsymbol{p}_h, \mathcal{G}_h^{\partial K}(u - \hat{u}_h)$ are all functions in $\mathcal{P}^k(K)$, it follows that:

$$\nabla u_h = -\boldsymbol{p}_h + \mathcal{G}_h^{\partial K}(u_h - \hat{u}_h).$$

Thus, we deduce that:

$$\|\nabla u_h\|^2_{L^2(\Omega;K)} = \| -\boldsymbol{p}_h + \mathcal{G}_h^{\partial K}(u_h - \hat{u}_h)\|^2_{L^2(\Omega;K)} \lesssim \|\boldsymbol{p}_h\|^2_{L^2(\Omega;K)} + \|\mathcal{G}_h^{\partial K}(u_h - \hat{u}_h)\|^2_{L^2(\Omega;K)}.$$

The conclusion is easy to drawn by Lemma 5.1. □

Another estimate derived from (5.10a) is the quantitative relationship between $\boldsymbol{p}_h$ and $\mathcal{L}_h^{\mathcal{CR}}(\bar{\hat{u}}_h)$.

Lemma 5.5. Given $(u_h, \hat{u}_h) \in \mathcal{X}_h^k$ and assuming $\boldsymbol{p}_h$ satisfies (5.10a), then:

$$\|\nabla \mathcal{L}_h^{\mathcal{CR}}(\bar{\hat{u}}_h)\|_{L^2(\Omega;K)} \le \|\boldsymbol{p}_h\|_{\boldsymbol{L}^2(\Omega;K)} \tag{5.14}$$

in each element K.

Proof. Selecting $\boldsymbol{q}_h = \nabla \mathcal{L}_h^{\mathcal{CR}}(\bar{\hat{u}}_h)$ in (5.10a) and noting that $\mathcal{L}_h^{\mathcal{CR}}(\bar{\hat{u}}_h) \in \mathcal{P}^1(K)$ implies $\nabla \mathcal{L}_h^{\mathcal{CR}}(\bar{\hat{u}}_h)$ is a constant vector in K. Hence,

$$\nabla \cdot \left(\nabla \mathcal{L}_h^{\mathcal{CR}}(\bar{\hat{u}}_h)\right) = 0.$$

Consequently, (5.10a) simplifies to:

$$(\boldsymbol{p}_h, \nabla \mathcal{L}_h^{\mathcal{CR}}(\bar{\hat{u}}_h))_K = -\langle \hat{u}_h, \nabla \mathcal{L}_h^{\mathcal{CR}}(\bar{\hat{u}}_h) \cdot \boldsymbol{n} \rangle_{\partial K}.$$

Given that $\nabla \mathcal{L}_h^{\mathcal{CR}}(\bar{\hat{u}}_h) \cdot \boldsymbol{n}$ is also constant, it follows that:

$$(\boldsymbol{p}_h, \nabla \mathcal{L}_h^{\mathcal{CR}}(\bar{\hat{u}}_h))_K = -\langle \bar{\hat{u}}_h, \nabla \mathcal{L}_h^{\mathcal{CR}}(\bar{\hat{u}}_h) \cdot \boldsymbol{n} \rangle_{\partial K} = -\langle \mathcal{L}_h^{\mathcal{CR}}(\bar{\hat{u}}_h), \nabla \mathcal{L}_h^{\mathcal{CR}}(\bar{\hat{u}}_h) \cdot \boldsymbol{n} \rangle_{\partial K} = -\|\nabla \mathcal{L}_h^{\mathcal{CR}}(\bar{\hat{u}}_h)\|^2_{\boldsymbol{L}^2(\Omega;K)},$$

with the final equality due to integration by parts. Applying the Cauchy-Schwarz inequality to the left-hand side yields the lemma's statement. □

We immediately obtain the following theorems in terms of $\boldsymbol{p}_h$ which are variants of Theorem 3.6 and Theorem 4.4. The proof follows directly by incorporating Lemma 5.4 and Lemma 5.5 into these theorems.

Theorem 5.6. Let $(u_h, \hat{u}_h) \in \mathcal{X}_h^k$, and $\boldsymbol{p}_h$ is obtained solved through (5.10a), then the following Poincaré inequalities hold:

$$\|u_h\|^2_{L^2(\Omega;\mathcal{T}_h)} \lesssim (1 + (h_K)^2)\|\boldsymbol{p}_h\|^2_{\boldsymbol{L}^2(\Omega;\mathcal{T}_h)} + h_K\|u_h - \hat{u}_h\|^2_{L^2(\Omega;\partial\mathcal{T}_h)} + \left(\int_\Omega \mathcal{L}_h^{\mathcal{CR}}(\bar{\hat{u}}_h)\, dx\right)^2 \tag{5.15}$$

and

$$\|u_h\|^2_{L^2(\Omega;\mathcal{T}_h)} \lesssim (1 + (h_K)^2)\|\boldsymbol{p}_h\|^2_{\boldsymbol{L}^2(\Omega;\mathcal{T}_h)} + h_K\|u_h - \hat{u}_h\|^2_{L^2(\Omega;\partial\mathcal{T}_h)} + \left(\int_\Gamma \hat{u}_h\, ds\right)^2 \tag{5.16}$$

where Γ is combination of boundary faces that has a positive measure, namely, $\Gamma = \bigcup_{i=1}^N e_i$ such that $e_i \in \partial\mathcal{T}_h^b$ and $\{e_1, e_2, \cdots, e_N\}$ are different boundary faces. In addition, the following variant of (5.15) expressing in term of integral of u_h also holds:

$$\|u_h\|^2_{L^2(\Omega;\mathcal{T}_h)} \lesssim (1 + (h_K)^2)\|\boldsymbol{p}_h\|^2_{\boldsymbol{L}^2(\Omega;\mathcal{T}_h)} + h_K\|u_h - \hat{u}_h\|^2_{L^2(\Omega;\partial\mathcal{T}_h)} + \left(\int_\Omega u_h\, dx\right)^2 \tag{5.17}$$

Theorem 5.7. Let $(u_h, \hat{u}_h) \in \mathcal{X}_h^k$, and $\boldsymbol{p}_h$ is obtained solved through (5.10a), then the following trace inequalities hold:

$$\|u_h\|^2_{L^2(\Omega;\partial\mathcal{T}_h^b)} \lesssim (1 + h_K)\|\boldsymbol{p}_h\|^2_{\boldsymbol{L}^2(\Omega;\mathcal{T}_h)} + \|u_h - \hat{u}_h\|^2_{L^2(\Omega;\partial\mathcal{T}_h)} + \left(\int_\Gamma \hat{u}_h\, ds\right)^2 \tag{5.18}$$

and

$$\|\hat{u}_h\|^2_{L^2(\Omega;\partial\mathcal{T}_h^b)} \lesssim (1 + h_K)\|\boldsymbol{p}_h\|^2_{\boldsymbol{L}^2(\Omega;\mathcal{T}_h)} + \|u_h - \hat{u}_h\|^2_{L^2(\Omega;\partial\mathcal{T}_h)} + \left(\int_\Gamma \hat{u}_h\, ds\right)^2, \tag{5.19}$$

where Γ is combination of boundary faces that has a positive measure, namely, $\Gamma = \bigcup_{i=1}^N e_i$ such that $e_i \in \partial\mathcal{T}_h^b$ and $\{e_1, e_2, \cdots, e_N\}$ are different boundary faces.

5.4. **Stability Analysis.** To the end, we address an application of the mathematical tools developed in this study to examine the stability of the HDG formulation (5.10) for the mixed boundary Poisson equation, specifically when the stabilization term is chosen to be a constant.

A crucial inquiry we pursue is whether it is possible to obtain an energy estimate for the HDG solution that does not depend on the mesh size h_K, without assuming additional regularity for the solution to the Poisson equation beyond the minimum requirements for the data f, u_D, and u_N. Existing research typically assumes the existence of a solution in a "strong" sense (with varying interpretations of "strong") and employs a projection-based analysis to verify the numerical solution's stability [24]. In a previous work [46], we initially proved the stability of the numerical solution with only minimal regularity, utilizing a translation argument. In this paper, our objective is to demonstrate the same result using a distinct approach, leveraging the mathematical instruments we have developed and making it easier to adapt to other type of problems.

More specifically, we seek to determine: for a given mesh $\mathcal{T}_h$, can $\|u_h\|_{L^2(\Omega;\mathcal{T}_h)}$ and $\|\boldsymbol{p}_h\|_{\boldsymbol{L}^2(\Omega;\mathcal{T}_h)}$ be uniformly bounded by a constant solely dependent on the input data and independent of the mesh size? This question is affirmatively addressed in the subsequent theorem:

Theorem 5.8. Let $(\boldsymbol{p}_h, u_h, \hat{u}_h) \in \boldsymbol{\mathcal{V}}_h^k \times \mathcal{U}_h^k \times \mathcal{F}_h^k$ solve (5.10) with $f \in L^2(\Omega), u_D \in L^2(\Gamma_D), u_N \in L^2(\Gamma_N)$, then the following estimate hold:

$$\|\boldsymbol{p}_h\|^2_{\boldsymbol{L}^2(\Omega;\mathcal{T}_h)} + \tau\|u_h - \hat{u}_h\|^2_{L^2(\Omega;\partial\mathcal{T}_h)} + \|\hat{u}_h\|^2_{L^2(\Omega;\Gamma_D)} \le C(f, u_D, u_N) \tag{5.20}$$

where the constant $C(f, u_D, u_N)$ depends on $\|f\|_{L^2(\Omega)}, \|u_D\|_{L^2(\Gamma_D)}, \|u_N\|_{\Gamma_N}$ and the domain but independent of the mesh.

Proof. Recall Lemma 5.3, the following identity hold:

$$\|\boldsymbol{p}_h\|^2_{\boldsymbol{L}^2(\Omega;\mathcal{T}_h)} + \tau\|u_h - \hat{u}_h\|^2_{L^2(\Omega;\partial\mathcal{T}_h)} = (f, u_h)_{\mathcal{T}_h} + \langle u_N, \hat{u}_h\rangle_{\Gamma_N}. \tag{5.21}$$

We firstly assume that Γ_D has a positive measure. In this case, the only thing we need to do is to bound $\|u_h\|_{L^2(\Omega;\mathcal{T}_h)}$ and $\|\hat{u}_h\|_{L^2(\Omega;\Gamma_N)}$ as

$$|(f, u_h)_{\mathcal{T}_h} + \langle u_N, \hat{u}_h\rangle_{\partial\mathcal{T}_h}| \le \|f\|_{L^2(\Omega)}\, \|u_h\|_{L^2(\Omega;\mathcal{T}_h)} + \|u_N\|_{L^2(\Gamma_N)}\, \|\hat{u}_h\|_{L^2(\Omega;\Gamma_N)}.$$

Choosing Γ in the Poincaré inequality (5.16) and the trace inequality (5.19) both to be Γ_D. As

$$\left(\int_{\Gamma_D} \hat{u}_h\, ds\right)^2 \le |\Gamma_D|\, \left(\int_{\Gamma_D} (\hat{u}_h)^2\, ds\right) = |\Gamma_D|\, \|\hat{u}_h\|^2_{L^2(\Omega;\Gamma_D)},$$

we can rewrite (5.16) and (5.19) as

$$\begin{aligned} \|u_h\|^2_{L^2(\Omega;\mathcal{T}_h)} &\lesssim (1 + h_K^2)\|\boldsymbol{p}_h\|^2_{\boldsymbol{L}^2(\Omega;\mathcal{T}_h)} + h_K\|u_h - \hat{u}_h\|^2_{L^2(\Omega;\partial\mathcal{T}_h)} + \left(\int_{\Gamma_D} \hat{u}_h\, ds\right)^2 \\ &\lesssim \|\boldsymbol{p}_h\|^2_{\boldsymbol{L}^2(\Omega;\mathcal{T}_h)} + \tau\|u_h - \hat{u}_h\|^2_{L^2(\Omega;\partial\mathcal{T}_h)} + \|\hat{u}_h\|^2_{L^2(\Omega;\Gamma_D)} \end{aligned} \tag{5.22}$$

and

$$\begin{aligned} \|\hat{u}_h\|^2_{L^2(\Omega;\partial\mathcal{T}_h^b)} &\lesssim (1 + h_K)\|\boldsymbol{p}_h\|^2_{\boldsymbol{L}^2(\Omega;\mathcal{T}_h)} + \|u_h - \hat{u}_h\|^2_{L^2(\Omega;\partial\mathcal{T}_h^b)} + \left(\int_{\Gamma} \hat{u}_h\, ds\right)^2 \\ &\lesssim \|\boldsymbol{p}_h\|^2_{\boldsymbol{L}^2(\Omega;\mathcal{T}_h)} + \tau\|u_h - \hat{u}_h\|^2_{L^2(\Omega;\partial\mathcal{T}_h)} + \|\hat{u}_h\|^2_{L^2(\Omega;\Gamma_D)} \end{aligned} \tag{5.23}$$

Using these estimates, together with (5.21) and (5.10c) with $\hat{v}_h = \hat{u}_h$, we get

$$\begin{aligned} &\|\boldsymbol{p}_h\|^2_{\boldsymbol{L}^2(\Omega;\mathcal{T}_h)} + \tau\|u_h - \hat{u}_h\|^2_{L^2(\Omega;\partial\mathcal{T}_h)} + \|\hat{u}_h\|^2_{L^2(\Omega;\Gamma_D)} \\ &= (f, u_h)_{\mathcal{T}_h} + \langle u_N, \hat{u}_h\rangle_{\Gamma_N} + \langle u_D, \hat{u}_h\rangle_{\Gamma_D} \\ &\lesssim \left(\|f\|_{L^2(\Omega)} + \|u_N\|_{L^2(\Gamma_N)} + \|u_D\|_{L^2(\Gamma_D)}\right)\left(\|\boldsymbol{p}_h\|^2_{\boldsymbol{L}^2(\Omega;\mathcal{T}_h)} + \tau\|u_h - \hat{u}_h\|^2_{L^2(\Omega;\partial\mathcal{T}_h)} + \|\hat{u}_h\|^2_{L^2(\Omega;\Gamma_D)}\right)^{\frac{1}{2}} \end{aligned}$$

It gives the desired estimate (5.20).

When $|\Gamma_D| = 0$, the scenario simplifies to a pure Neumann problem. According to classical elliptic theory, the solution to a Neumann problem is unique up to a constant [41]. Hence, to ensure uniqueness in the numerical scheme, one could introduce an additional condition such as:

$$\int_{\partial\Omega} \hat{u}_h\, ds = 0 \qquad \text{or} \qquad \int_{\Omega} u_h\, dx = 0.$$

Incorporating this condition into the numerical scheme eliminates the arbitrary constant, thereby securing a unique solution. The analysis procedure previously discussed remains applicable, as the Poincaré and trace inequalities would work to derive (5.20). The details are omitted here to avoid redundancy, as it repeats the earlier process. □

Acknowledgements

We are grateful for the valuable discussions with Guosheng Fu, Jay Gopalakrishnan, Jiannan Jiang, and Noel Walkington. We also extend our thanks to the National Science Foundation (grant number: NSF DMS-1929284) for their support of this research.

References

[1] R. Altmann and C. Carstensen. P_1-nonconforming finite elements on triangulations into triangles and quadrilaterals. *SIAM Journal on Numerical Analysis*, 50(2):418–438, 2012.

[2] T. Apel, S. Nicaise, and J. Schöberl. Crouzeix-Raviart type finite elements on anisotropic meshes. *Numerische Mathematik*, 89:193–223, 2001.

[3] D. N. Arnold. Mixed finite element methods for elliptic problems. *Computer methods in applied mechanics and engineering*, 82(1-3):281–300, 1990.

[4] D. N. Arnold and F. Brezzi. Mixed and nonconforming finite element methods: implementation, postprocessing and error estimates. *ESAIM: Mathematical Modelling and Numerical Analysis*, 19(1):7–32, 1985.

[5] D. N. Arnold and R. Winther. Mixed finite elements for elasticity. *Numerische Mathematik*, 92:401–419, 2002.

[6] L. Botti, D. A. Di Pietro, and J. Droniou. A hybrid high-order method for the incompressible Navier–Stokes equations based on temam's device. *Journal of Computational Physics*, 376:786–816, 2019.

[7] S. Brenner and L.-Y. Sung. Piecewise H^1 functions and vector fields associated with meshes generated by independent refinements. *Mathematics of Computation*, 84(293):1017–1036, 2015.

[8] S. C. Brenner. Poincaré–Friedrichs inequalities for piecewise H^1 functions. *SIAM Journal on Numerical Analysis*, 41(1):306–324, 2003.

[9] S. C. Brenner. *The mathematical theory of finite element methods*. Springer, 2008.

[10] S. C. Brenner. Forty years of the Crouzeix-Raviart element. *Numerical Methods for Partial Differential Equations*, 31(2):367–396, 2015.

[11] A. Buffa and C. Ortner. Compact embeddings of broken Sobolev spaces and applications. *IMA journal of numerical analysis*, 29(4):827–855, 2009.

[12] E. Burman, O. Duran, and A. Ern. Hybrid high-order methods for the acoustic wave equation in the time domain. *Communications on Applied Mathematics and Computation*, 4(2):597–633, 2022.

[13] Z. Cai, J. Douglas, and X. Ye. A stable nonconforming quadrilateral finite element method for the stationary Stokes and Navier-Stokes equations. *Calcolo*, 36, 12 2000.

[14] G. Chen, D. Han, J. R. Singler, and Y. Zhang. On the superconvergence of a hybridizable discontinuous Galerkin method for the Cahn–Hilliard equation. *SIAM Journal on Numerical Analysis*, 61(1):83–109, 2023.

[15] G. Chen, P. Monk, and Y. Zhang. An HDG method for the time-dependent drift–diffusion model of semiconductor devices. *Journal of Scientific Computing*, 80(1):420–443, 2019.

[16] P. G. Ciarlet. *The finite element method for elliptic problems*. SIAM, 2002.

[17] B. Cockburn. The hybridizable discontinuous Galerkin methods. In *Proceedings of the International Congress of Mathematicians 2010 (ICM 2010) (In 4 Volumes) Vol. I: Plenary Lectures and Ceremonies Vols. II–IV: Invited Lectures*, pages 2749–2775. World Scientific, 2010.

[18] B. Cockburn, D. A. Di Pietro, and A. Ern. BriDGing the hybrid high-order and hybridizable discontinuous Galerkin methods. *ESAIM: Mathematical Modelling and Numerical Analysis*, 50(3):635–650, 2016.

[19] B. Cockburn, G. Fu, and W. Qiu. A note on the devising of superconvergent HDG methods for Stokes flow by M-decompositions. *IMA Journal of Numerical Analysis*, 37(2):730–749, 2017.

[20] B. Cockburn, G. Fu, and W. Qiu. Discrete H^1-inequalities for spaces admitting M-decompositions. *SIAM Journal on Numerical Analysis*, 56(6):3407–3429, 2018.

[21] B. Cockburn and J. Gopalakrishnan. A characterization of hybridized mixed methods for second order elliptic problems. *SIAM Journal on Numerical Analysis*, 42(1):283–301, 2004.

[22] B. Cockburn, J. Gopalakrishnan, and R. Lazarov. Unified hybridization of discontinuous Galerkin, mixed, and continuous Galerkin methods for second order elliptic problems. *SIAM Journal on Numerical Analysis*, 47(2):1319–1365, 2009.

[23] B. Cockburn, J. Gopalakrishnan, N. Nguyen, J. Peraire, and F.-J. Sayas. Analysis of HDG methods for Stokes flow. *Mathematics of Computation*, 80(274):723–760, 2011.

[24] B. Cockburn, J. Gopalakrishnan, and F.-J. Sayas. A projection-based error analysis of HDG methods. *Mathematics of Computation*, 79(271):1351–1367, 2010.

[25] B. Cockburn, J. Guzmán, and H. Wang. Superconvergent discontinuous Galerkin methods for second-order elliptic problems. *Mathematics of Computation*, 78(265):1–24, 2009.

[26] B. Cockburn, J. R. Singler, and Y. Zhang. Interpolatory HDG method for parabolic semilinear PDEs. *Journal of Scientific Computing*, 79:1777–1800, 2019.

[27] M. Crouzeix and P.-A. Raviart. Conforming and nonconforming finite element methods for solving the stationary Stokes equations I. *Revue française d'automatique informatique recherche opérationnelle. Mathématique*, 7(R3):33–75, 1973.

[28] D. Di Pietro and J. Droniou. A hybrid high-order method for Leray–Lions elliptic equations on general meshes. *Mathematics of Computation*, 86(307):2159–2191, 2017.

[29] D. Di Pietro and A. Ern. Discrete functional analysis tools for discontinuous Galerkin methods with application to the incompressible Navier–Stokes equations. *Mathematics of Computation*, 79(271):1303–1330, 2010.

[30] D. Di Pietro and S. Lemaire. An extension of the Crouzeix–Raviart space to general meshes with application to quasi-incompressible linear elasticity and Stokes flow. *Mathematics of Computation*, 84(291):1–31, 2015.

[31] D. A. Di Pietro and J. Droniou. The hybrid high-order method for polytopal meshes. *Number 19 in Modeling, Simulation and Application*, 2020.

[32] D. A. Di Pietro and A. Ern. *Mathematical aspects of discontinuous Galerkin methods*, volume 69. Springer Science & Business Media, 2011.

[33] D. A. Di Pietro and A. Ern. A hybrid high-order locking-free method for linear elasticity on general meshes. *Computer Methods in Applied Mechanics and Engineering*, 283:1–21, 2015.

[34] D. A. Di Pietro and R. Tittarelli. An introduction to hybrid high-order methods. *Numerical Methods for PDEs: State of the Art Techniques*, pages 75–128, 2018.

[35] Z. Ding. A proof of the trace theorem of Sobolev spaces on Lipschitz domains. *Proceedings of the American Mathematical Society*, 124(2):591–600, 1996.

[36] Z. Dong and A. Ern. Hybrid high-order and weak Galerkin methods for the biharmonic problem. *SIAM Journal on Numerical Analysis*, 60(5):2626–2656, 2022.

[37] J. Droniou and L. Yemm. Robust hybrid high-order method on polytopal meshes with small faces. *Computational Methods in Applied Mathematics*, 22(1):47–71, 2022.

[38] S. Du and F.-J. Sayas. New analytical tools for HDG in elasticity, with applications to elastodynamics. *Mathematics of Computation*, 89(324):1745–1782, 2020.

[39] A. Ern, J.-L. Guermond, et al. *Finite elements II*. Springer, 2021.

[40] L. Esposito, C. Nitsch, and C. Trombetti. Best constants in Poincaré inequalities for convex domains. *Journal of Convex Analysis*, 20:253–264, 01 2013.

[41] L. C. Evans. *Partial differential equations*, volume 19. American Mathematical Society, 2022.

[42] R. Eymard, T. Gallouët, and R. Herbin. Finite volume methods. *Handbook of numerical analysis*, 7:713–1018, 2000.

[43] G. Fu, B. Cockburn, and H. Stolarski. Analysis of an HDG method for linear elasticity. *International Journal for Numerical Methods in Engineering*, 102(3-4):551–575, 2015.

[44] D. Gilbarg, N. S. Trudinger, D. Gilbarg, and N. Trudinger. *Elliptic partial differential equations of second order*, volume 224. Springer, 1977.

[45] P. Hansbo and M. G. Larson. Discontinuous Galerkin and the Crouzeix–Raviart element: application to elasticity. *ESAIM: Mathematical Modelling and Numerical Analysis*, 37(1):63–72, 2003.

[46] J. Jiang, N. J. Walkington, and Y. Yue. Stability and convergence of HDG schemes under minimal regularity. *arXiv preprint arXiv:2310.18448*, 2023.

[47] V. John et al. *Finite element methods for incompressible flow problems*, volume 51. Springer, 2016.

[48] F. Kikuchi. Rellich-type discrete compactness for some discontinuous Galerkin FEM. *Japan journal of industrial and applied mathematics*, 29(2):269–288, 2012.

[49] R. M. Kirby, S. J. Sherwin, and B. Cockburn. To CG or to HDG: a comparative study. *Journal of Scientific Computing*, 51:183–212, 2012.

[50] K. Kirk. Numerical analysis of space-time hybridized discontinuous Galerkin methods for incompressible flows. 2022.

[51] K. Kirk, A. Çeşmelioğlu, and S. Rhebergen. Convergence to weak solutions of a space-time hybridized discontinuous Galerkin method for the incompressible Navier–Stokes equations. *Mathematics of Computation*, 92(339):147–174, 2023.

[52] J. Nečas. Les méthodes directes en théorie des équations elliptiques. *Academia*, 1967.

[53] N. C. Nguyen, J. Peraire, and B. Cockburn. An implicit high-order hybridizable discontinuous Galerkin method for linear convection–diffusion equations. *Journal of Computational Physics*, 228(9):3232–3254, 2009.

[54] N. C. Nguyen, J. Peraire, and B. Cockburn. An implicit high-order hybridizable discontinuous Galerkin method for nonlinear convection–diffusion equations. *Journal of Computational Physics*, 228(23):8841–8855, 2009.

[55] N. C. Nguyen, J. Peraire, and B. Cockburn. A hybridizable discontinuous Galerkin method for Stokes flow. *Computer Methods in Applied Mechanics and Engineering*, 199(9-12):582–597, 2010.

[56] N. C. Nguyen, J. Peraire, and B. Cockburn. An implicit high-order hybridizable discontinuous Galerkin method for the incompressible Navier–Stokes equations. *Journal of Computational Physics*, 230(4):1147–1170, 2011.

[57] L. E. Payne and H. F. Weinberger. An optimal Poincaré inequality for convex domains. *Archive for Rational Mechanics and Analysis*, 5(1):286–292, 1960.

[58] J. Peraire and P.-O. Persson. The compact discontinuous Galerkin (cDG) method for elliptic problems. *SIAM Journal on Scientific Computing*, 30(4):1806–1824, 2008.

[59] W. Qiu, J. Shen, and K. Shi. An HDG method for linear elasticity with strong symmetric stresses. *Mathematics of Computation*, 87(309):69–93, 2018.

[60] B. Rivière. *Discontinuous Galerkin methods for solving elliptic and parabolic equations: theory and implementation*. SIAM, 2008.

[61] R. Sevilla and A. Huerta. Tutorial on hybridizable discontinuous Galerkin (HDG) for second-order elliptic problems. In *Advanced finite element technologies*, pages 105–129. Springer, 2016.

[62] J. Shen. Hybridizable discontinuous Galerkin method for nonlinear elasticity. 2017.

[63] A. Ten Eyck and A. Lew. Discontinuous Galerkin methods for non-linear elasticity. *International Journal for Numerical Methods in Engineering*, 67(9):1204–1243, 2006.

[64] M. Vohralík. On the discrete Poincaré–Friedrichs inequalities for nonconforming approximations of the Sobolev space H^1. *Numerical functional analysis and optimization*, 26(7-8):925–952, 2005.

[65] T. Warburton and J. S. Hesthaven. On the constants in hp-finite element trace inverse inequalities. *Computer methods in applied mechanics and engineering*, 192(25):2765–2773, 2003.

[66] J. Wloka. *Partial differential equations*. Cambridge University Press, 1987.

[67] O. C. Zienkiewicz, R. L. Taylor, and J. Z. Zhu. *The finite element method: its basis and fundamentals*. Elsevier, 2005.

(Yukun Yue)
University of Wisconsin Madison, Madison, USA.
Email address: yyue@math.wisc.edu